Technische Universität München
Fakultät für Physik

Abschlussarbeit im Bachelorstudiengang Physik

Leptogenesis: A Non-Relativistic Study

Leptogenese: Eine nicht-relativistische Betrachtung

Tobias Theil

25th July 2017

Erstgutachter (Themensteller): Dr. Antonio Vairo
Zweitgutachter: Prof. Dr. Sherry Suyu

Contents

1. Introduction

One of todays greatest unsolved mystery is the observed asymetry between baryons and antibaryons in the known universe. A useful way to quantify this asymmetry is by using

$$\eta = \frac{n_b - n_{\bar{b}}}{n_\gamma} = \frac{n_B}{n_\gamma}, \tag{1.1}$$

where n_b and $n_{\bar{b}}$ are the number densities of baryons and antibaryons respectively, $n_B = n_b - n_{\bar{b}}$ and n_γ the photon density. Using the fact that in the visible universe nearly no antimatter is observed, leads to $n_b - n_{\bar{b}} \simeq n_b$ and therefore

$$\eta \simeq \frac{n_b}{n_\gamma}. \tag{1.2}$$

Although measuring the exact value of η is impossible because this would include counting all baryons and antibaryons in the whole universe there are two ways to obtain a range of values for η, namely using the model of Big Bang Nucleosynthesis (BBN) and the Cosmic Microwave Background (CMB)[1]. In the first case the primordial abundances of the four stable isotopes formed during BBN, namely D, ^{3}He, ^{4}He and ^{7}Li, that are observed, are compared to the η-dependent values of these abundances predicted by the theoretical BBN model, resulting in [2, Eq. (1.25)]

$$4.7 \times 10^{-10} \leq \eta \leq 6.5 \times 10^{-10}. \tag{1.3}$$

On the other hand a more precise way of probing the baryon asymmetry is by using the CMB or more precisely any anisotropies showing in the otherwise isotropic spectrum. Analyzing these anisotropies gives a pretty precise result of [2, Eq. (1.26)]

$$\eta = (6.1 \pm 0.16) \times 10^{-10}, \tag{1.4}$$

which is in the range for η given above.

Now the most intuitive way to introduce this asymmetry to the universe is to set it as a initial condition, meaning by assuming the universe already started in an asymmetric state. This initial abundance, however, would be diluted so much by the inflation of the universe described by the in many other ways successful big bang theory, leaving behind no significant baryon asymmetry. One could also argument, that the universe is strictly symmetric considering baryon number, but that matter and antimatter are concentrated in big domains throughout the universe, which come into contact just at their outer borders. This would lead to big gamma bursts at their borders due to annihilation of matter and antimatter that would greatly disturb the isotropic nature of the CMB. Since no kind of such distortions are observed it is safe to say that such big clusters of antimatter do not exist or they have to be at least as big as the presently observable universe[3]. Interesting to note is that even with a completly symmetric universe there would still be some baryons and antibaryons present, their number density, however, would be extremely Boltzmann suppressed resulting in

$$\frac{n_b}{n_\gamma} \approx \frac{n_{\bar{b}}}{n_\gamma} \approx 10^{-18}, \tag{1.5}$$

which is eight orders of magnitude below the observed value given in (1.4).

Putting all this together leads to the necessity of a theory in which the universe is initially matter-antimatter symmetric and the asymmetry is generated dynamically over time. This can happen via baryon number violating processes that produce the baryon asymmetry and therefore induce the so called baryogenesis. On the other hand a lepton number asymmetry can be produced by the CP-violating decay of heavy, sterile neutrionos that will than be transformed into a baryon number asymmetry by baryon plus lepton number violating processes. This whole process, that was first proposed by Fukugita and Yanagida[4], is called baryogenesis via leptogenesis.

The outline of this thesis then is the following: Chapter 2 will introduce the basic principles of baryogenesis and how these principles can and cannot be realised in the current Standard Model (SM) of particle phyics. Chapter 3 will then focus on how to extend the SM in order to sucessfully adopt a scenario in which the baryon asymmetry is produced by baryogenesis through leptogenesis. Chapter 4 then quantitatively describes leptogenesis using Boltzmann equations in a non-relativistic regime and takes lowest order relativistic and radiative corrections into account. Chapter 5 finally shows the numerical results of the rate equations introduced in chapter 4 as well as the effect of the relativisticcorrections as well as the importance of the usage of the correct statistics.

Chapter 4 and 5 closely follow [5] and [6].

2. Outline of baryogenesis

One way to describe the observed baryonic asymmetry is by assuming that the universe has been in an asymmetric state just from the beginning and that the matter and antimatter is concentrated in big domains throughout the universe, which come into contact just at their outer borders. Techincally, there is no reason for the universe not to have started in an asymmetric state, but in that case one would measure high gamma rates due to the matter-antimatter-annihilation right between these distinct regions.

Since there is no such radiation observed, patches of different kinds of matter have to be as big as the presently observable universe. Because this doesn't seem very plausible, the baryonic asymmetry had to arise dynamically from an universe where matter and antimatter existed in the same amount.

Actually, in 1967 Andrei Sakharov postulated the criteria, which have to be met in order for an excess of baryons over anti-baryons to be generated out of a fully symmetrical universe.

2.1. Sakharov Conditions

As mentioned above, there are three crucial properties of nature, the Sakharov conditions, which are required to produce a net baryon number greater than zero. These three conditions are:

1. B-violating process(es)
2. C and CP violation
3. Departure from or loss of thermal equilibrium

For a general insight into these three conditions the first one will be skipped, since it is quite obvious that in a totally symmetric universe there has to be at least one B-violating process in order to cause an imbalance in matter and antimatter. The general importance of the other two will be discussed in the following.

2.1.1. C and CP-violation

C symmetry states that physical processes are the same, even after exchanging particles for their respective anti-particles, while P-symmetry guarantees invariance under the transformation $\vec{r} \to -\vec{r}$. CP symmetry then simply is a sequence of a C followed by a P transformation.

To explain both C and CP have to be violated for baryogenesis beeing possible, one has to keep in mind that any state consisting of baryon number carrying particles changes the sign of its baryon number under C- as well as under CP-transformations[7, p. 4]. This means that the only C and CP invariant states are the ones with a zero baryon number, just like our assumed initially symmetrical universe. This implies that the baryon number in the universe stays zero, unless C and CP are violated[7, p. 4].

2.1.2. Departure from thermal equilibrium

The last condition to be met in order for baryogenesis to be achievable is that the the B, C and CP violating processes must occur outside the thermal equilibrium. To illustrate this we first

consider the thermal distribution of a species X of quantum particles

$$f(E_X) = \frac{1}{e^{\frac{E_X - \mu_X}{T}} \pm 1}, \tag{2.1}$$

where the plus sign stands for fermions and the minus sign for bosons, respectively. The energy E_X and the momentum $\vec{p}_X$ are related via the relativistic energy-momentum-relation $E_X^2 = \vec{p}_X^2 + m_X^2$. μ_X describes the chemical potential of the particle species X, which is an important quantity for describing thermal equilibrium states, as the chemical potentials of two species X and Y, which are in thermal equilibrium, are related by $\mu_X = \mu_Y$ or for more species $\sum_i \mu_i = 0$.

Using eq. (2.1) to compute the particle density of a certain particle species one gets

$$n_X = g_X \int \frac{d^3p}{(2\pi)^3} f_X(E), \tag{2.2}$$

where g_X denotes the number of inner degrees of freedom of X.

For heavy particles m_X is of order E_X and it holds $m_X \gg T$. With this approximation the denominator of the exponential function in eq. (2.1) gets small compared to the numerator so the exponential itself gets so big that the ± 1 can be neglected: In the non-relativistic limit, you get the same particle density for fermions and bosons. By dividing E_X into the rest energy m_X and the kinetic energy $\mathrm{E}_{\mathrm{kin}}$ and after approximating

$$E_{\mathrm{kin}} \approx \frac{p^2}{2m}, \tag{2.3}$$

for non-relativistic particles, integrating according to (2.2) yields

$$n_X = g_X \frac{4\pi}{(2\pi)^3} \int dp\, p^2 e^{\frac{\mu_X - m_X}{T}} e^{-\frac{p^2}{2m_X T}} = g_X \left(\frac{m_X T}{2\pi}\right)^{\frac{3}{2}} e^{-\frac{m_X - \mu_X}{T}}. \tag{2.4}$$

Analogously one gets the number density for the corresponding anti-particle $\bar{\mathrm{X}}$

$$n_{\bar{X}} = g_{\bar{X}} \left(\frac{m_{\bar{X}} T}{2\pi}\right)^{\frac{3}{2}} e^{-\frac{m_{\bar{X}} - \mu_{\bar{X}}}{T}}. \tag{2.5}$$

Now suppose X and its anti-particle $\bar{\mathrm{X}}$ with $\mathrm{B}_X = -\mathrm{B}_{\bar{X}} \neq 0$ are in thermal equilibrium then the condition $\mu_X = \mu_{\bar{X}}$ holds. Comparing eq. (2.4) and (2.5) one sees that the chemical potential is the only property that could differ for particles and antiparticles. Now using the equilibrium condition for chemical equilibrium, one finally gets

$$n_X = n_{\bar{X}}. \tag{2.6}$$

Looking at equation (2.6) it is obvious that even with B, C and CP violation any produced excess baryon number B will be washed out in equilibrium by other processes happening in equilibrium.

This illustrates the final Sakharov condition, that next to B, C and CP violation a departure from equilibrium is needed for a dynamic production of excess baryons.

Interesting to note is that there is quite an easy way of approximately determining if reactions take place in thermal equilibrium, namely by comparing the reaction rate with the expansion of the universe, described by the Hubble constant H, which is actually not a constant but changes with time. So if the relation

$$\Gamma \gtrsim H \tag{2.7}$$

holds, the reactions take place fast enough for them to be in equilibrium. This can be made understandable, by looking at this from the rest frame of the particles taking part in the reactions. Then the particles do not notice any expansion of the universe since they move and react too fast with each other: the expansion does not really affect the equilibrium state.

Otherwise, if the reactions occur slower than the universe expands, meaning

$$\Gamma < H \tag{2.8}$$

is valid, then the expansion happens fast enough that particles get separated too far from each other, so they cannot react anymore and the reactions fall out of equilibrium.

2.2. Baryogenesis in the Standard Modell

Although nowadays there are no records or experimental proofs on earth for baryon number violating processes, that does not mean there is a need for physics beyond the Standard Modell (SM) of particle physics, at least on a qualitative level.

2.2.1. The $SU(2)_L$x$U(1)_Y$ symmetry of the SM

As it turns out, the electroweak part of the SM with its $SU(2)_L \times U(1)_Y$ symmetry groups suits best for describing baryogenesis. But before the way this is achieved in the SM is displayed, this section will give a short rundown on the $SU(2)_L \times U(1)_Y$ symmetry found in the SM.

The $U(1)_Y$ symmetry can be represented by the following transformations:

$$\Psi \longrightarrow e^{i\frac{Y}{2}\alpha(x)}\Psi,$$
$$\bar{\Psi} \longrightarrow e^{-i\frac{Y}{2}\alpha(x)}\bar{\Psi},$$

with Ψ a Dirac spinor, $\bar{\Psi} = \gamma^0\Psi^\dagger$, with γ^0 one of the gamma matrices and $\alpha(x)$ being an arbitrary function. Y denotes the $U(1)_Y$ quantum number, the hypercharge. Because of the exponential nature of this transformation to check for $U(1)_Y$-symmetry, the hypercharges of all appearing particles in each term of the Lagrangian must add up to zero.

The $SU(2)_L$ symmetry however acts just on left-handed particles with the transformation looking like

$$\begin{pmatrix} u_L \\ d_L \end{pmatrix} \longrightarrow U(x) \begin{pmatrix} u_L \\ d_L \end{pmatrix},$$

where U(x)=$e^{i\theta^i(x)T^i}$ with T^i=$\sigma^i/2$ the weak isospin. It should be noticed that u and d in the transformation above stand for all up-type particles (ν_e,ν_μ,ν_τ,u,c,t) respectively all down-type particles (e,μ,τ,d,s,b). The right-handed particles on the other hand transform as singlets under $SU(2)_L$

$$X_R \longrightarrow X_R,$$

where X_R stands for any right-handed SM particle. Using this simple transformation one can easily deduce that for right-handed particles $T = T_3$=0.

Also there is a simple relation that connects the hypercharge Y, the electrical charge Q and the third component of the isospin T_3:

$$Q = T_3 + \frac{Y}{2}. \tag{2.9}$$

2.2.2. Electroweak baryogenesis

As stated above, the electroweak sector of the SM has every ingredient needed for successfull baryogenesis. The following discussions will illustrate how the SM satisfies all three Sakharov conditions.

C and CP violation

It is already proven theoretically und experimentally by numerous well-known experiments, for example the Wu experiment in 1956, that P symmetry is maximally violated by the weak interaction in the leptonic as well as in the hadronic sector. As shown by Kobayashi and Maskawa through expanding the Cabibbo hypothesis and experimentally confirmed, weak interactions in the hadronic sector also violate CP invariance, which manifests as an complex phase in the CKM quark mixing matrix. In the leptonic sector however the CP violation through a complex phase only got postulated in the Pontecorvo-Maki-Nakagawa-Sakata (PMNS) neutrino mixing matrix trying to describe neutrino oscillations, but this phase still needs to be measured.

Nevertheless the elektroweak part of the SM, more precise the weak interactions, since electromagnetism does not violate C or even P, satisfies at least one of the three Sakharov conditions.

B violation

Although the first Sakharov condition, the necessity of baryon number violating processes, seems to be the most obvious, the way these are realised in the SM is not obvious because of non-perturbative processes.

Since at the classical level baryonic and, as it is going to play an important role during the following discussion, the leptonic currents are conserved

$$\partial^\mu J^B_\mu = 0, \tag{2.10}$$

$$\partial^\mu J^L_\mu = 0, \tag{2.11}$$

one would assume that the SM could not produce a baryon asymmetry. However, by considering quantum fluctuation, meaning orders higher than just tree level, one finds that the currents for the left- and right-handed parts f_L and f_R respectively, where f stands for quarks and leptons equally, are not conserved and furthermore not the same [8]

$$\partial^\mu \bar{f}_L \gamma_\mu f_L = -c_L \frac{g^2}{32\pi^2} F^a_{\mu\nu} \tilde{F}^{a\mu\nu}, \tag{2.12}$$

$$\partial^\mu \bar{f}_R \gamma_\mu f_R = +c_R \frac{g^2}{32\pi^2} F^a_{\mu\nu} \tilde{F}^{a\mu\nu}, \tag{2.13}$$

where g denotes the gauge coupling, $F^{a\mu\nu}$ the field tensor, $\tilde{F}^{a\mu\nu}$ the dual field tensor and c_L and c_R depend on the representation of f_L and f_R.This behaviour of the currents at quantum levels is known as Adler-Bell-Jackiw or chiral anomaly. Since $\mathrm{SU}(2)_L$ gauge boson only couples with left-handed particles c^W_R=0, while the $\mathrm{U}(1)_Y$ gauge boson couples to both handednesses, but with different strength, therefore $\mathrm{c}^Y_R \neq \mathrm{c}^Y_L$. Although this section only focuses on electroweak baryogenesis, it is mentionable that the $\mathrm{SU}(3)_c$ gauge bosons of the strong interactions do not produce any chiralty anomaly because they couple with left as well as right-handed particles with the same strenght, so $\mathrm{c}^c_R = \mathrm{c}^c_L$ and both currents in (2.12) and (2.13) cancel each other out in the case of strong interactions.

Putting this and equations (2.10) - (2.13) together, gives

$$\partial^\mu J^B_\mu = \partial^\mu J^L_\mu = \frac{n_F}{32\pi^2}\left(-g_w^2 W^a_{\mu\nu}\tilde{W}^{a\mu\nu} + g'^2 B_{\mu\nu}\tilde{B}^{\mu\nu}\right), \tag{2.14}$$

with $W^{a\mu\nu}$ and $B^{\mu\nu}$ the field strenght tensors of the $\mathrm{SU}(2)_L$ and $\mathrm{U}(1)_Y$ gauge groups,$\tilde{W}^{a\mu\nu}$ and $\tilde{B}^{\mu\nu}$ the respective dual tensors and n_F=3 the number of particle families.

Analyzing equation (2.14) one easily figures out that although baryon and lepton number are not conserved separately the difference B-L of these numbers is very well conserved. Integrating both sides of eq. (2.14), as shown in [8, pp. 15f.], results in

$$\Delta B = \Delta L = n_F \Delta N_{CS}, \tag{2.15}$$

where ΔN_{CS} is the difference of the so called Chern-Simons numbers. How exactly these numbers are derived and what their integral representation is can also be looked up in [3, 7, 8], but is not of great interest for this thesis. However, one property of these numbers is quite relevant for baryon asymmetry, namely that each integer valued Chern-Simons number describes one distinct vacuum state of the infinite electroweak vacua with minimal energy, which are separated by a potential barrier. The difference of these numbers of two vacuum states right next to each other is $\Delta \mathrm{N}_{CS} = \pm 1$, so changing from one vacuum state N_i to another N_f results in $\Delta \mathrm{N}_{CS} \neq 0$ and therefore a change in baryon and lepton number is induced. Also interesting to notice is, since the number of particle families n_F=3 baryon and lepton numbers change at least by three units each.

The last question regarding B violation in the SM is about how such a transition between two vacuum states can be accomplished. One way is through a quantummechanical effect called the instaton, where the system simply tunnels through the barrier between two vacuum states with different Cher-Simons numbers. However 't Hooft, the one showing B vioaltion can happen through the chiral anomaly, also showed [8, p. 18] that the cross section for such a tunneling process is about

$$\sigma \propto e^{-\frac{4\pi}{\alpha_w}} \sim 10^{-164}, \tag{2.16}$$

with $\alpha_w = \frac{g^2}{4\pi} \cong \frac{1}{30}$. This cross section is so small that such a instaton transition between two vacua probably does not happen even once during the whole lifetime of the universe.

A second way such a change of vacua can be induced is through the so called sphaleron processes. The requirement for these processes to take place is that the system has enough energy to go over the potential barrier instead of tunneling through. The minimum energy needed, known as the spaleron energy, is about[3, 8]

$$E_{sph} = \frac{4\pi}{g_2} v(T) \cong 8 - 13\mathrm{TeV}, \tag{2.17}$$

where the temperature dependent quantity $v(\mathrm{T})$ describes the vacuum expectation value of the Higgs field at the temperature T, which will be important later on.

In fact this kind of processes are quite possible for temperatures above 100 GeV, however, below this temperature the rate of spaleron processes is exponentially suppressed by a Boltzmann factor.On the other hand, comparing the sphaleron rate for temperatures above 100 GeV, which are proportional to the fourth power of the temperature [8, p. 19], with the Hubble constant, gives information about when these processes are in thermal equilibrium and numerical evaluations yield that the sphaleron processes are in thermal equilibrium for

$$100\mathrm{GeV} \lesssim T \lesssim 10^{12}\mathrm{GeV}.$$

So as shown in section 2.1.2, even though the SM provides the necessary tools for C, CP and B violation, below the temperature of around 10^{12} GeV any produced net baryon number will be washed out and below 100 GeV the temperature is far below the temperature needed to induce sphaleron processes.

Departure from thermal equilibrium and elecroweak phase transistion

The final question to answer regarding baryogenesis in the SM is how the last Sakharov condition, the departure from thermal equilibrium is realized. The most common way is by using the electroweak phase transition.

This phenomenon relies on the vacuum expectation value (VEV) of the $\mathrm{SU}(2)_L$ Higgs doublet and its behaviour during the early times of the universe. At the present day the VEV is greater than zero, which leads to a gauge symmetry breaking and therefore masses of any fermion, the electroweak bosons and the Higgs bososn. But it has already been shown [8, p. 21] that for high temperatures the VEV of the universe equals zero and the $\mathrm{SU}(2)_L \times \mathrm{U}(1)_Y$ gauge symmetry is still intact. This obviously means that at some point during the evolution of the universe and at some temperature $T = T_c$ the VEV changed from zero to non-zero, or in other words a phase transition from a totally symmetrical phase to a phase with broken symmetry occured at some point. In order to generate a departure from thermal equilibrium for the B violating reaction this transition must be strongly of first order, meaning at $T = T_c$ the VEV changes discontinuously from zero to non-zero.

Just as with cooling steam this process can be imagined with bubbles of phases with broken symmetries forming and expanding inside the phase of unbroken symmetry, like droplets of water form in the vapor and expand, until they connect and finally cover all space. Now, the way this phase transition leads to a baryon asymmetry is as follows.

First of all, consider a thin wall, so that the area where quarks and fermions interact with the walls can be approximated as a step function. Also, to simplify matters, assume that the expansion of the bubbles of broken symmetry is spherical symmetric, therefore this problem can be reduced to one dimension[8, p. 33]

At the start of this baryon asymmetry generating process there is the same amount of particles and anti-particles.

While the bubble expands, left- and right-handed quarks and anti-quarks from the unbroken phase hit the bubble wall, get reflected under CP violating processes and change their helicity due to angular momentum conservation and since charge conservation holds (anti-)quarks are only allowed to scatter into (anti-)quarks. The scattering processes are the following:

$$\begin{aligned} q_L &\to q_R, \\ q_R &\to q_L, \\ \bar{q}_L &\to \bar{q}_R, \\ \bar{q}_L &\to \bar{q}_R. \end{aligned}$$

Since these scattering processes are not CP conserving the reflection coefficents are not the same for all of the reactions above:

$$\Delta R = R_{\bar{L}\to\bar{R}} - R_{R\to L} = R_{\bar{R}\to\bar{L}} - R_{L\to R}. \tag{2.18}$$

Using CPT invariance yields

$$R_{\bar{L}\to\bar{R}} = R_{L\to R}, \tag{2.19}$$

$$R_{\bar{R}\to\bar{L}} = R_{R\to L}. \tag{2.20}$$

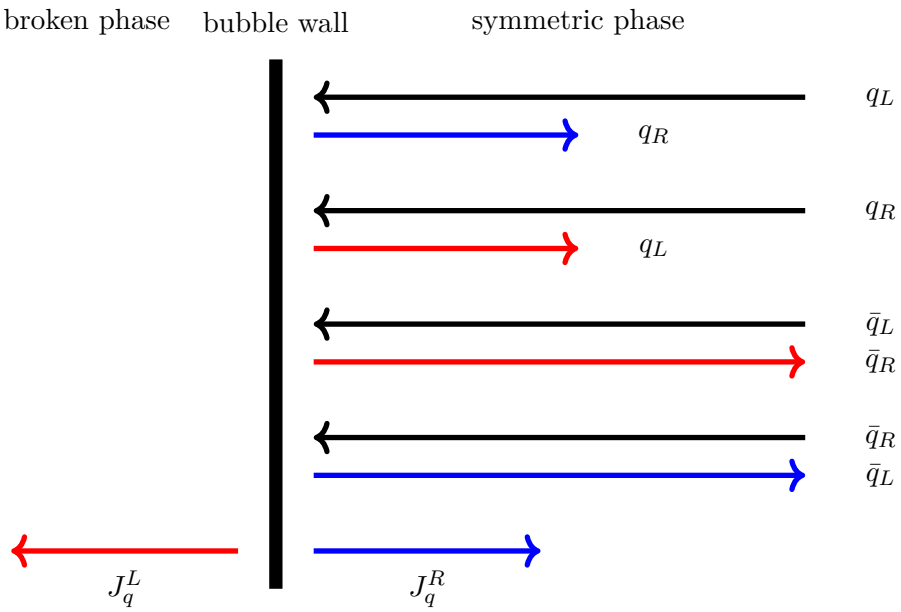

Figure 2.1.: Reflection of quarks and anti-quarks with different helicities respectively at a bubble wall. The length of the arrows of the reflected particles represents the flux of the respective particle. The effect of CP violation was chosen arbitrarily, by inverting it only the signs of the difference currents J_q^L and J_q^R would change but they would still cancel each other.

These relations alone imply that there still is no net baryon number, since the differences J_q^L of the fluxes of $\bar{q}_R$ and q_L and the J_q^R of q_R and $\bar{q}_L$ reflected back into the symmetric phase are the same and cancel each other out, as depicted in figure 2.1. Now taking into account the weak (B+L) violating sphaleron processes changes only J_q^L while J_q^R stays the same, since weak forces only interact with left-handed particles and right-handed anti-particles. These processes then change the baryon number to a value $\Delta B \neq 0$ near the bubble wall and this baryon number gets frozen in after the bubble sweeps over this particular area because in the broken phase the (B+L) violating processes are strongly Boltzmann suppressed [8]. This means that the only factor responsible for the sign of the baryon number are the sphaleron processes. In particular this means that every bubble of broken phase contributes with the same sign to the whole baryon number and no two or more bubbles cancel each other out, because the sphaleron processes everywhere act the same way. The way these have to work in order to produce a positive baryon number is shown in section 5.4 of [8].

2.2.3. Failures of the SM

Since the SM offers everything needed to describe baryogenesis in the early universe, from B via C and CP violation to departures from the thermal equillibrium during the electroweak phase transition of possibly first order, one could naively say that the only thing left is the experimental proof to be delivered.

Having said this, recent experiments have shown that the SM alone, is not able to provide a strong enough phase transition of first order or more precisely a phase transition of first order at all. This will be shown in the following.

First, the reason why a strong first order transition is needed for baryogenesis is the following [8, p. 25]: Only for a strong first order phase transition the transition itself happens rapidly enough to keep up with the particle reactions and to induce a out-of-equilibrium state that way.

According to the Landau theory phase transitions are described by the behaviour of an order parameter. So for a first order phase transition the order parameter has to change dicontinuously at the critical point, while for a second order transition the order parameter has to change drastically as well, but this change occurs continuously. The way the order of the phase transition can be determinded is by introducing the order parameter as a new variable to the effective potential describing the free energy of the system which can be Taylor expanded with respect to the order parameter and temperature dependent coefficients in the vicinity of the phase transition, because here the order paramter ist small. The next step is to minimize the free energy with respect to the order parameter. If at some temperature the free energy shows two degenerated minima a first order phase transitions occurs because the transition from one minimum, or ground state, to another has to happen discontinously. If there are not more than one minima at a certain temperature but the ground state changes anyway a continuous phase transiton of higher order occured.

In a case of the electroweak phase transition the order parameter ist the expectation value of the Higgs field denoted as v and the potential describes the energy of a system in a state with the Higgs expectation value v. Since in general this state is not one of minimal energy and because every system prefers to minimize its energy, it changes into a state described by the minimum of the potential where the expectation value of the Higgs is by definition the Higgs VEV.

As it is already known, the Higgs VEV had to change from zero at the big bang to a non-zero value while the universe cools down to the temperature measured nowadays, so it is just natural to look at the change of this value with temperature. As discribed above, the change of the VEV can now happen continunously in which case the system undergoes a second order phase transition or discontinuously what is needed for a first order transition and especially for elektroweak baryogenesis. Both cases are shown in figure 2.2 for the effective Higgs potential

$$V_{\text{eff}} = D(T^2 - T_0)^2\phi^2 - ET\phi^3 - \frac{1}{4}\lambda\phi^4, \tag{2.21}$$

,including one-loop corrections [7] for different non-zero temperature regimes. D and E are constant factors which are not relevant for this discussion and λ describes the 4-Higgs self coupling.

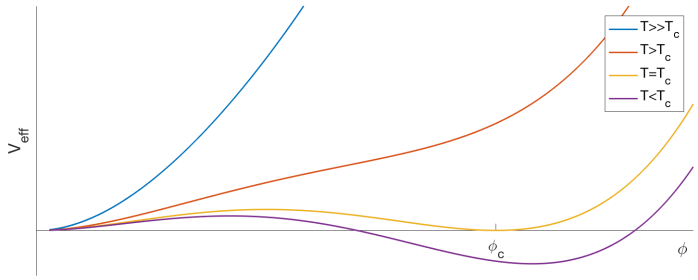

(a) Effective Higgs field for first order transition

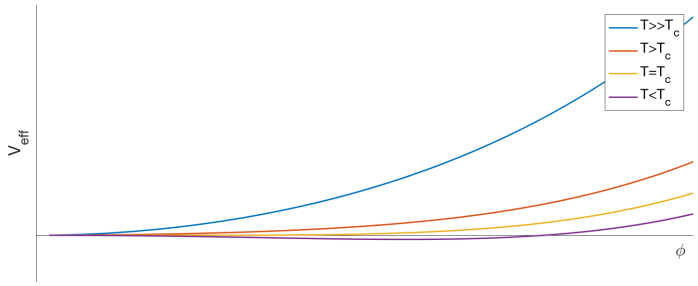

(b) Effective Higgs field for second order transition

Figure 2.2.: Effective Higgs field for different phase transitions

Figure 2.2(a) clearly shows the first order characteristics of the phase transition. While for high temperatures the VEV equals zero for the highly symmetric phase, the potential slowly develops a second minimum for decreasing temperature until at the critical temperature T=T$_c$ there are two energetically degenerated mimima, one at ϕ_1=0 and one at ϕ_2=ϕ_c, which are separated by an energy barrier. However, the system can change from the minimum at ϕ_1 to the one at ϕ_2 resulting in a discontinuous change of the VEV and therefore inducing a first order phase transition. While the universe keeps on cooling down because of the universe's expansion, the new minimum gets energetically lowered while the original one stays at V_{eff}=0 and thus becomes a maximum, leaving an unstable state where once was a symmetric vacuum state. Since in both cases the new ground state does not have the same symmetry as original one, this phenomenon is called spontaneous symmetry breaking.

How this can be imagined in the early universe is that at some point in space and time the universe changed from one minimun to another thus breaking the symmetry locally and producing a local bubble of broken phase. These bubbles get bigger with time and combine with other bubbles whose generation gets much more likely as the temperatures lowers the barrier between the minima and increase the tunneling probability.

On the other hand, figure 2.2(b) shows how the universe would develop in case of a second order transition. In this case even at T=T$_c$ there are no two degenerated minima but the new one develops gradually while the orignial minimum more and more becomes the unstable maximum you also get in figure 2.2(a) for low temperatures. Since there are no two minima the universe can choose between, there is also no bubble formation but instead a continuous condensation throughout the universe which is not enough to induce baryogenesis.

Now that the two possibilities of the electroweak phase transition were represented the question how and why the SM fails to provide a strong enough first order phase transition still needs to be answered.

To do this it is useful to define a quantity that corresponds to the strenght of the phase

transistion, which in this case will be

$$\frac{v_{T_c}}{T_c} \gtrsim 1. \tag{2.22}$$

The reason why (2.22) is a good way to represent the strength of the phase transition is that by using equation (2.17) and the fact that the B+L violating sphaleron processes are exponentially surpressed by a Boltzmann factor inside of the phases with broken symmetry one gets for the rate of these spalerons at the critical temperature

$$\Gamma_{\text{sphaleron}} \propto e^{-E_{\text{sph}}(T_c)/T_c} \propto e^{-v_{T_c}/T_c}. \tag{2.23}$$

So equation (2.23) really shows that the spaleron rates inside the bubbles with a Higgs VEV greater than zero are suppressed exactly by the quantity given in (2.22). So in order for these processes to be suppressed adequately, v_{T_c}/T_c has to be at least 1, which results in a suppression factor of roughly 0.36, for the phase transition to be strong enough to cause baryogenesis.

There are various methods to use the condition in (2.23) in order to calculate the Higgs mass and what the biggest mass is the Higgs particle can have in order for a first order phase transition to be possible which results in about m_H<70 GeV [9, pp. 3f.].

This theoretical result together with the experimental discovery that the Higgs mass is greater than 114 GeV [10, pp. 100ff.] clearly shows that the electroweak phase transition and therefore the SM as a whole is not able to explain how the observed baryonic asymmetry arose during the early times of the universe.

A solution for this problem is extending the SM in such a way that the new elements are able to explain problems the SM was not able to. One of these extensions results in leptogenesis, which will be the topic of the following sections.

3. Outline of leptogenesis

As stated in the section before, the SM alone is not quite enough to describe the observed baryon abundance, so the SM has to be expanded to the effect that it can describe such phenomena.

A possible extension of the SM that explains baryogenesis is baryogenesis via leptogenesis. The key idea here is to introduce a heavy, right-handed Majorana neutrino N, whose decays violate lepton number conservation.

This and the following chapter will cover this concept in some detail.

3.1. Expanding the SM

There are experimental reasons to extend the SM in the neutrino sector , namely the results of neutrino oscillation experiments. These oscillations are only possible if the neutrinos are not massless. Making things complicated is the fact that only left-handed neutrinos have been observed, meaning adding massive neutrinos to the SM cannot be done in the same way as for the other fermions, since they are Dirac fermions that appear as left- as well as right-handed fields. To circumvent this problem, without adding new degrees of freedom to the SM, one could assume that neutrinos are Majorana particles, meaning particle and anti-particle are the same, leading to a mass term of the form [11]

$$\mathcal{L}_{N,M} = -\frac{1}{2}\overline{N^c} M^M N, \tag{3.1}$$

with N the Majorana field describing the neutrino and where the superscript C stands for the charge conjugated neutrino field defined by

$$N^c \equiv C\bar{N}^T,$$

with the charge conjugation marix C, which is dependent on the representation of the gamma matrices. The Majorana mass M^M is an $\mathrm{n}_F \times \mathrm{n}_F$ matrix with n_F the number of neutrino families.

To show that this mass term can be constructed just by using left-handed fields the Dirac representation of the gamma matrices will be used, resulting in a charge conjugaton matrix of the form

$$C = i\gamma^2\gamma^0, \tag{3.2}$$

with

$$\gamma^2 = \begin{pmatrix} 0 & \sigma^2 \\ -\sigma^2 & 0 \end{pmatrix} \quad ; \quad \gamma^0 = \begin{pmatrix} 1 & 0 \\ 0 & -1 \end{pmatrix}$$

and σ^2 one of the Pauli matrices. Now by using the left-handed component, obtained by using the left-handed projector given in appendix A.1,

$$\psi_L \equiv P_L\psi, \tag{3.3}$$

where ψ is an abritrary spinor, one can construct a Majorana field just by using ψ_L:

$$\psi_M = \begin{pmatrix} \psi_L \\ i\sigma^2\psi_L^* \end{pmatrix}$$

$$\Rightarrow \psi_M^c = \begin{pmatrix} -i\sigma^2(i\sigma^2\psi_L^*)^* \\ i\sigma^2\psi_L^* \end{pmatrix} = \begin{pmatrix} \psi_L \\ i\sigma^2\psi_L^* \end{pmatrix} = \psi_M$$

Before concluding this section there are a few interesting things worth mentioning regardng the Majorana mass term. First, such a term would violate lepton number conservation because it violates the global SM symmetry

$$\Psi \xrightarrow{U(1)} e^{i\ell\alpha}\Psi, \tag{3.4}$$

which can easily be seen in

$$\overline{N^c}N \xrightarrow{U(1)} \overline{(e^{i\ell\alpha}N)^c}e^{i\ell\alpha}N = \overline{e^{-i\ell\alpha}N^c}e^{i\ell\alpha}N = e^{i\ell\alpha}\overline{N^c}e^{i\ell\alpha}N \neq \overline{N^c}N.$$

This symmetry however is connected to the lepton number [8, p. 14], so breaking it directly results in non-conservation of lepton number. This seems rather obvious because if Majorana particles are particles and anti-particles at the same time one cannot assing them a distinct lepton number and therefore it is not conserved.

The second interesting to note thing is how a Majorana mass term like the one given in (3.1) arises in the Lagrangian. Because all mass terms would break the SM gauge symmetry if added directly to the Lagrangian, so there has to be some other way. For Dirac particles such a term arises from the Yukawa coupling term of a fermion field to the scalar Higgs field, similar to the one given in (3.19). The mass term then enters the Lagrangian via spontaneous symmetry breaking for temperatures below the critical temperature for the electroweak phase transition described above. Similarly the Majorana mass term originates from some coupling of the participating fields and the Higgs field to enter the Lagrangian afer spontaneous symmetry breaking. This coupling however is not the Yukawa coupling but of the form [11, Eq. (5)]

$$\frac{1}{\Lambda}\left(\frac{1}{2}\overline{\ell_L}\tilde{\phi}f\tilde{\phi}^T\ell_L^c + h.c.\right), \tag{3.5}$$

with some flavor matrix f and some energy scale Λ. The operator in parentheses is of dimension 5 which is why the parameter Λ has to be introduced. This parameter describes the energy scale of physics beyond the SM.

3.2. The seesaw Mechanism

Introducing the mass terms of neutrinos to the Lagrangian after the electroweak symmetry breaking results in [11, pp. 4f]

$$\begin{aligned}\mathcal{L} = \mathcal{L}_{SM} + i\bar{N}_I\partial\!\!\!/\nu_I - (m^D)_{\alpha I}\bar{\nu}_\alpha N_I - (m^D)^*_{\alpha I}\bar{N}_I\nu_\alpha \\ - \frac{1}{2}\left[(M^M)_{IJ}\overline{N^c}_I N_J + (M^M)^*_{IJ}\bar{N}_{R,I}N^c_J\right].\end{aligned} \tag{3.6}$$

This can be rewritten as[11, Eq. (12)]

$$\mathcal{L}_{M+D} = \left(\overline{\nu}, \overline{N^c}\right)\begin{pmatrix} 0 & m^D \\ m^D & M_R^M \end{pmatrix}\begin{pmatrix} \nu^c \\ N \end{pmatrix} + h.c.\ . \tag{3.7}$$

The matrix m^D contains the masses of a typical lepton like the electron, while M^M describes the Majorana mass. The matrix above as a whole is of the dimension
$(n_f + n_M) \times (n_f + n_M)$ with n_f the number of observable neutrino flavours and n_M the number of flavours of their right-handed counterparts.

Although the addition of neutrino masses can be described using the mass term (**??**) there is still a problem, namely why the neutrino masses are many orders of magnitude smaller than those of the other SM particles. This however can be described using the so called seesaw mechanism. In this discussion only the so called type I seesaw mechanism will be presented. By doing so the following two assumptions have to be made:

1. The Dirac masses arise directly from the Higgs mechanism that gives mass to all SM particles and is of order of a typical lepton or quark in the SM.

2. The Majorana masses are much bigger than the Dirac masses, $\mathrm{m}^D \ll \mathrm{M}^M$. This mass scale arises from GUT's and is of order $\sim 10^{10} - 10^{16}$ GeV.

The subscript R will be dropped from now on since there is no non-zero left-handed Majorana mass and therefore no further distinction is needed.

Now, after diagonalising the mass matrix in (3.7) [12, pp. 2-3], one gets two mass eigenvalues, in particular

$$M_1 \backsimeq -m^D \left(M^M\right)^{-1} \left(m^D\right)^T,$$
$$M_2 \backsimeq M^M,$$

or for just one neutrino family

$$M_1 \backsimeq -\frac{m_D^2}{M^M}, \tag{3.8}$$
$$M_2 \backsimeq M^M. \tag{3.9}$$

Now finding the corresponding eigenstates to these eigenvalues results in linear combinations of ν and N.

$$n_1 = \nu \cos\phi - N^c \sin\phi, \tag{3.10}$$
$$n_2 = \nu \sin\phi + N^c \cos\phi, \tag{3.11}$$

with their charge conjugated forms

$$n_1^c = \nu^c \cos\phi - N \sin\phi, \tag{3.12}$$
$$n_2^c = \nu \sin\phi + N \cos\phi. \tag{3.13}$$

Since the mixing angle ϕ is of order m_D/M and $m_D \ll M$, $\phi \ll 1$ and therefore one can expand the sines and cosines in (3.10)-(3.13) and gets

$$n_1 \approx \nu, \tag{3.14}$$
$$n_1^c \approx \nu^c, \tag{3.15}$$
$$n_2 \approx N^c, \tag{3.16}$$
$$n_2^c \approx N. \tag{3.17}$$

Putting all this back into the mass term of the Lagrangian yields at leading order

$$\mathcal{L}_{mass} \approx -\overline{n_1} M_1 n_1^c - \overline{n_2} M_2 n_2^c + h.c.\,. \tag{3.18}$$

Seeing that the first as well as the second term of this Lagrangian only consist of left- and right-handed neutrinos respectively implies that these are Majorana mass terms and therefore by applying the seesaw mechanism to the SM one gets two Majorana neutrinos, n_1 and n_2.

Since $n_1 \approx \nu$ at leading order in ϕ this mass eigenstate mostly left-handed and with a mass M_1 very light, suggesting that this is the light neutrino observable today.

On the other hand because $n_2 \approx N^c$ this mass eigenstate is mostly right-handed and very heavy with a mass of M_2, so it cannot be detected other as via gravitational effects. This heavy right-handed neutrino is also the prime candidate for enabling baryogenesis via leptogenesis.

Interesting to note is how these two masses behave under changing M^M. It is quite obvious from equation (3.8) that by raising the large mass scale and as a consequence thereof raising the mass of the heavy neutrino the mass of the light neutrinos gets even lower and vice versa, hence the name seesaw mechanism.

3.3. Leptogenesis and the Sakharov conditions

After the necessary expansion of the SM was performed in the previous section, this section will focus on how the right-handed, heavy neutrinos are able to produce a net, non-zero baryon number, that is how the Sakharov conditions can be fulfilled using this extended SM.

In the following discussions the assumption that three heavy right-handed neutrinos exist will be made. In addition, it is required that the masses of these neutrions are hierarchical in the sense that $M_1 \ll M_{2,3}$ and that only the lightest of these neutrinos actually play a significant role for leptogenesis.

The key ingredient for baryogenesis via leptogenesis is the decay of the heavy, right-handed neutrinos introduced above, that is described by the following Yukawa interaction term:

$$\mathcal{L}_{\mathrm{N,Yuk}} = h_{ij}\overline{N_i}\tilde{\phi}^\dagger l_j + h_{ij}^* \overline{l_i}\tilde{\phi} N_j. \tag{3.19}$$

The h_{ij} describe the complex Yukawa couplings, the ℓ_i are the left-handed lepton SU(2) doublets of the Standard model and $\tilde{\phi} \equiv i\sigma^2\phi^*$ is the isospin conjugate of the Higgs doublet. It can be shown that this additional term does not violate the symmetries of the SM Lagrangian. This interaction term will be analyzed in more detail in Appendix A.

The Feynman diagrams for both decay channels are depicted in figure 3.1. The right-handed neutrinos being Majorana particles as a result of the seesaw mechanism do not preserve lepton number and because of this they can decay into leptons as well as anti-leptons, as it can be seen in figure 3.1.

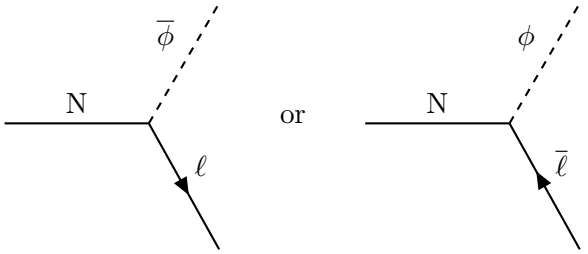

Figure 3.1.: Feynman diagrams for the N-decay

B violation

The B violation in the frame of leptogenesis is achieved in the same way as in direct electroweak baryogenesis via the B+L violating sphaleron processes. Because of the net lepton number

asymmetry produced by N decays this means that the lepton abundance is converted into a baryon abundance by these processes.

C and CP violation

The CP violation for the N_1 decay comes from the complex nature of the Yukawa couplings introduced in equation (3.19). This coupling then violates CP by interfering Feynman diagrams for this decay, tree level decay, however, are not enough to produce any CP violation since the complex phases of h_{ij} cancel each other out by taking the square of any interference because only one neutrino flavour appears in tree level decays. Because of this at leas one loop diagrams with intermediate states of neutrinos of different flavour have to be interfered with the tree level decay, so the phases do not cancel each other out. This then contributes to CP violation since the CP-conjugated decay then is not the same as the unconjugated one. The necessary one-loop diagrams are depicted in figure 3.2.

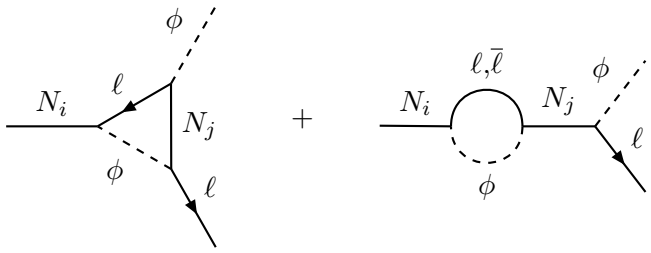

Figure 3.2.: One-loop diagrams for the N-decay

Here it can be seen clearly that a distinction between N_i and N_j has to be made since the virtual neutrinos transmissioned during these processes are not of the same flavour as the neutrino in the initial state. This means that in order for CP to be violated there has to exist at least an extra neutrino next to the lightest one.

This being said, one can calculate the CP asymmetry[13, pp. 24ff.], which is in general defined as

$$\epsilon = \frac{\Gamma(N_1 \to \bar{\phi}\bar{\ell}) - \Gamma(N_1 \to \phi\ell)}{\Gamma(N_1 \to \bar{\phi}\bar{\ell}) + \Gamma(N_1 \to \phi\ell)}, \tag{3.20}$$

by interfering the tree level decay with the one-loop decays. By assuming hierarchical heavy neutrino masses the CP violation can be expressed as [**?**][Eq. (55)]Buchmuller:2005eh

$$\epsilon \simeq \frac{3}{16\pi} \frac{1}{(hh^\dagger)^2_{11}} \sum_{i=2,3} \mathrm{Im}\left[\left(hh^\dagger\right)^2_{i1}\right] \frac{M_1}{M_i} \tag{3.21}$$

For a certain choice of parameters this results in [13, p. 26]

$$\epsilon \gtrsim 10^{-6}, \tag{3.22}$$

which shows CP violation by the decay of heavy right-handed Majorana neutrinos.

Deviation from the equilibrium

The last condition that has to be met for successfull baryogenesis is that the decay of the heavy neutrinos must occur outside of equilibrium. For high enough temperatures, namely for $T \gtrsim M_1$, the decay of the neutrino is in equilibrium with the inverse decay $\phi\ell \to N$ and no net lepton number can be produced even if the other two conditions hold as shown in sec. 2.1.2. Even if

during inflation an abundance of N was produced the lepton asymmetry would be washed out by equilibrium processes as soon as the temperature rises up to at least the mass of the heavy neutrino during the reheating phase of the early universe.

However, if the temperature drops below M_1 the heavy neutrino inverse decay is exponentially suppressed by a Boltzmann factor because with falling temperature it becomes exponentially more unlikely for a lepton and Higgs to have enough energy to form a heavy neutrino, while the neutrinos themselves can still decay into lepton and Higgs. This means that decays happening before the neutrino density converges to the equilibrium density happen outside of equilibrium and a net lepton number can be produced, that, because of suppression of inverse decays, will not be washed out and as a consequence thereof will be transformed into a baryon abundance through the B+L violating electroweak sphaleron processes.

The requirement for the neutrino decay to be slow enough to sustain its out-of-equilibrium state is the following [14, p. 30].

$$\Gamma_D < H. \tag{3.23}$$

Γ_D denotes the total decay rate of the neutrinos while H is the expansion rate of the universe. This relation is equivalent to the one given in (2.8) as a requirement for processes to be out of equilibrium.

4. Analytic approximations and calculations

4.1. Rate equations for leptogenesis

In order to qualitatively describe leptogenesis one has to consider rate equations for the lepton number and B-L number densities. In a static universe without lepton number violating processes the rate equation would trivially be

$$\frac{d}{dt}n = 0. \tag{4.1}$$

If one now condsiders a universe expanding with the rate H the rate equation above changes to

$$\left(\frac{d}{dt} + 3H\right) n = 0. \tag{4.2}$$

Finally including lepton number violating processes the rate equation one obtains for the neutrino number density is

$$\left(\frac{d}{dt} + 3H\right) n_N = -\Gamma_N \left(n_N - n_N^{eq}\right) + \Gamma_{N,B-L} n_{B-L}. \tag{4.3}$$

Applying this reasoning to the B-L number density yields

$$\left(\frac{d}{dt} + 3H\right) n_{B-L} = \Gamma_{B-L,N} \left(n_N - n_N^{eq}\right) - \Gamma_{B-L} n_{B-L}. \tag{4.4}$$

The coefficient Γ_N denotes how fast the neutrino density equalizes with its equilibrium density, while Γ_{B-L} describes the washout of a net B-L number. $\Gamma_{B-L,N}$ describes how the B-L asymmetry is affected by the deviation of the neutrino density from its equilibrium value and together with $\Gamma_{N,B-L}$ these two coefficients characterize CP violating processes [5, p. 4]. Since both these coefficients describe CP violating processes they must depend on the CP violating parameter ϵ introduced in the section before and it was also shwon there that this parameter is small for heavy neutrino decays and because $n_{B-L} \ll \left(n_N - n_N^{eq}\right)$ the second term in equation (4.3) can be neglegted.

The goal now is to determine these coefficients at least at leading order and the first one will be Γ_N. To get this coefficient one has to integrate equation (4.3) over phase space, resulting in

$$\left(\frac{\partial}{\partial t} - Hp\frac{\partial}{\partial p}\right) f_N = \Gamma_N \left(e^{E_N/T} - f_N\right). \tag{4.5}$$

The whole calculation on how to perform the phase space integral can be found in appendix B.1.

One might now notice that equation (4.5) differs from equation 4 in [5] by a factor of $\mathrm{M}_N/\mathrm{E}_N$, that origins in a different normaliziation of the phase space. However, since we operate in a non-relativistic regime $\mathrm{E_N} \approx \mathrm{M_N}$, therefore this factor is ~ 1 and negligible. Using this argumentation one can also see that $\Gamma_N = \Gamma_0$ with Γ_0 the total decay rate of the heavy neutrinos, which is governed by the Yukawa interaction term (3.19). It has to be mentioned that for the equilibrium distribution the Boltzmann statistic with neglegted chemical potential was used since the energy of a neutrino $\mathrm{E_N} \approx \mathrm{M_N} \gg \mathrm{T}$ during the phase where the decay happen outside equilibrium and

therefore quantum mechanical effects play an insignificant role and can be neglected. Going back to the decay rate, that can be calculated as done in appendix A.2, one gets

$$\Gamma_N = \Gamma_0 = \frac{|h_{11}|^2 M_N}{8\pi}. \tag{4.6}$$

As explained above $\Gamma_{B-L,N}$ connects the B-L asymmetry with the deviation of n_N from its equilibrium value and because the only processes able to produce a B-L asymmetry are the decays of the heavy neutrino and therefore $\Gamma_{B-L,N}$ is directly connected to its decay rate. On the other hand though, any B-L asymmetry can only arise through CP violation, meaning the neutrino has to decay into leptons and anti-leptons at different rates. The parameter describing this difference is ϵ, as it is given in (3.20). Putting all this together results in

$$\Gamma_{B-L,N} = \epsilon\Gamma_0. \tag{4.7}$$

The last coefficient left to determine is Γ_{B-L}. This one however refers to the washout of the B-L asymmetry hence it arises from the inverse decay $\ell\phi \to N$. It can be calculated using the quatum field theoretical means for obtaining decay rates and taking into account that particle distributions and neutrino momenta have to be considered because of non-zero temperatures.

$$\Gamma_{B-L} n_{B-L} = \int \prod_{a=N,\ell,\phi} \frac{d^3 p_a}{2E_a(2\pi)^3} (2\pi)^4 \delta(p_\ell + p_\phi - p_N)(f_\ell f_\phi - f_{\bar{\ell}} f_{\bar{\phi}}) \sum |M_0|^2, \tag{4.8}$$

where $\sum |M_0|^2 = 16\pi M_N \Gamma_0$ describes the tree level matrix element for exactly this inverse decay summed over all spins of N and isospin components of ℓ. In order to evaluate this integral properly one has to first describe the term $(f_l f_\phi - f_{\bar{l}} f_{\bar{\phi}})$ more precisely. Since we operate at rather high temperatures one can use Boltzmann statistics for lepton and Higgs regardless and expanding in the chemical potentials up to first order yields.

$$f_\ell f_\phi - f_{\bar{\ell}} f_{\bar{\phi}} \simeq 2e^{-\frac{E_N}{T}} \frac{\mu_l + \mu_\phi}{T}. \tag{4.9}$$

As mentioned in [5, p. 7] the chemical potentials are proportional to the B-L number density and by using the coefficients c_l and c_ϕ in order to avoid introducing the exact temperature dependant relations one can also connect n_{B-L} to the lepton and Higgs asymmetries through [5, p. 7]

$$n_\ell - n_{\bar{\ell}} = -c_\ell n_{B-L}, \tag{4.10}$$

$$n_\phi - n_{\bar{\phi}} = -c_\phi n_{B-L}, \tag{4.11}$$

Different values for c_l and c_ϕ then correspond to different temperature ranges that are given in table 4.1[5, Table 1].

T (GeV)	c_l	c_ϕ
$\ll 10^{13}$	1	2/3
$\sim 10^{13}$	1	14/23
$10^{12} - 10^{13}$	3/4	1/2
$10^{12} - 10^{13}$	78/115	56/115
$10^{12} - 10^{13}$	344/537	52/179

Table 4.1.: Values of c_l and c_ϕ for different temperature ranges

Now by expanding the number distribution for leptons and Higgs and their respective anti

particles in the chemical potentials up to first order one can finally put the chemical potential and n_{B-L} in relation to each other. It is important to note that one has to use the Fermi-Dirac- and Bose-Einstein distribution for leptons and Higgses respectively. The reason for this is that these two particle species are in equilibrium at the temperature T. Because of this and the fact that they are relativistic particles, their kinetic energy and therefore momenta are of order T and quantum effects cannot be neglected. On the other hand it is possible to use Boltzmann statistics for leptons and Higgs bosons above since particles taking part in the production of a heavy neutrinos having energies or momenta of order $M_N/2 \gg T$ and quantum effects can safely be neglected in this case. Finally using quantum statistics results in

$$\mu_\ell = \frac{3c_l}{T^2} n_{B-L}, \tag{4.12}$$

$$\mu_\phi = \frac{3c_l}{2T^2} n_{B-L}. \tag{4.13}$$

Using all these results and putting them into relation (4.8) one gets the following result for the washout rate $\Gamma_{B\text{-}L}$

$$\Gamma_{B\text{-}L} = \frac{3}{\pi^2} \left(c_\ell + \frac{c_\phi}{2} \right) z^2 K_1(z) \Gamma_0, \tag{4.14}$$

with $K_1(z)$ the modified Bessel function of the second kind and

$$z \equiv \frac{M_N}{T}. \tag{4.15}$$

This can be seen as a dimensionless measure for time, since the temperature of the universe decreases over time and therefore z increases. The exact derivation of these results can be looked up in appendix B.2.

Using the relations given in (2.7) and (2.8) it is usefull to define the so called wash out factor K as follows

$$K \equiv \left. \frac{\Gamma_0}{H} \right|_{T=M_N}. \tag{4.16}$$

Using this and equation 3 of [15]

$$H(z) = H|_{T=M_N} \cdot \frac{1}{z^2}, \tag{4.17}$$

one can now compare the rates calculated above to the Hubble constant H.

For $T \lesssim M_N$ one can approximate Γ_N as Γ_0 resulting in

$$\frac{\Gamma_N}{H} \simeq \frac{\Gamma_0}{\frac{1}{z^2} H|_{T=M_N}} = z^2 K. \tag{4.18}$$

Since z increases with time, equation (4.18) clearly shows that the rate with which the neutrino number density approaches its equilibrium value gets greater than the expansion of the universe and therefore the deviation from equilibrium vanishes over time.

Looking at (4.14) one can easily see that for $T \sim M_N$, or $z \approx 1$, $\Gamma_{B\text{-}L}$ is of the same order as Γ_N, since $K_1(1)=\mathcal{O}(1)$. On the other hand however, for really low temperatures, meaning $T \ll M_N$ or z very big, one can see the quantitative behaviour of $\Gamma_{B\text{-}L}$ by using the asymptotic expansion of the modified Bessel function given by

$$K_n(z) \sim \sqrt{\frac{\pi}{2z}} e^{-z} \sum_{k=0}^{\infty} \frac{a_k(n)}{z^k},$$

with $a_k(n)$ some coefficients that are not of any interest for this matter. Now using this and dropping all but the first term of the sum above, which is justified because z is large, one gets

$$\frac{\Gamma_{B\text{-}L}}{H} \sim \sqrt{\frac{1}{z}} e^{-z} z^2 \frac{\Gamma_0}{\frac{1}{z^2} H|_{T=M_N}} = z^{\frac{7}{2}} e^{-z} K. \tag{4.19}$$

So because Γ_N increases with z for $z \approx 1$ so does $\Gamma_{B\text{-}L}$. However, as equation (4.19) suggests, $\Gamma_{B\text{-}L}$ gets more and more suppressed by the exponential factor for increasing z and therefore has to have some maximum. Additionally for sufficiently low temperatures, like the extremely low 2.7K of the present universe, the washouth rate $\Gamma_{B\text{-}L}$ is effectively zero and any symmetry produced in earlier times is frozen out. All this can be seen in figure 4.1 where the previously calculated ratios are plotted against z and are normalized to the washout factor K.

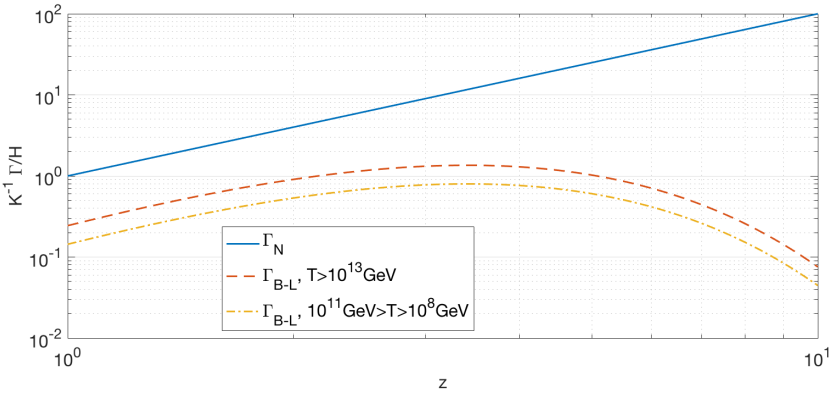

Figure 4.1.: The ratios Γ_N/H and $\Gamma_{B\text{-}L}/H$ plotted against H

4.2. Relativistic corections

Although this thesis focuses on a non-relativistic scenario for leptogenesis it might be interesting to see how much relativistic corrections influence the previous results. For this matter one has to reintroduce the factor M_N/E_N seen in equation 4 of [5], that was dropped in equation (4.5) since it simplifies to 1 in the non-relativistic limit, so this equation reads

$$\left(\frac{\partial}{\partial t} - Hp\frac{\partial}{\partial p}\right) f_N = \frac{M_N \Gamma_0}{E_N} \left(e^{E_N/T} - f_N\right). \tag{4.20}$$

Now, using the relativistic energy-momentum relation,

$$E = \sqrt{M^2 + p^2}, \tag{4.21}$$

one can expand the factor $1/E_N$ on the right-hand side up to order p^2 and therefore get the next-to-leading order relativisitic corrections for the rate equation (4.3)

$$\left(\frac{d}{dt} + 3H\right) n_N = \Gamma_N \left(n_N^{eq} - n_N\right) + \Gamma_{N,u} \left(u - u^{eq}\right), \tag{4.22}$$

with u the kinetic energy density of the heavy neutrinos divided by their mass

$$u = \frac{g_N}{M_N} \int \frac{d^3p}{(2\pi)^3} \frac{p^2}{2M_N} f_N, \tag{4.23}$$

with g_N the the internal degrees of freedom of the neutrinos.

By multiplying (4.22) with p^2 and integrating over p one can easily get a rate equation for u, which at leading order in p, so for E_N=M_N, reads as

$$\left(\frac{d}{dt} + 5H\right) u = \Gamma_u \left(u^{eq} - u\right). \tag{4.24}$$

It is important to note that for the rates appearing above, the following relations are holding

$$\Gamma_{N,u} = \Gamma_0, \tag{4.25}$$
$$\Gamma_u = \Gamma_0. \tag{4.26}$$

Now again by expanding the factor $1/E_N$ one gets an equivalent expansion for equation (4.4). Since the B-L asymmetry density is not directly affected by any relativistic effects, only the term containing the neutrino density has to be expanded, resulting in

$$\left(\frac{d}{dt} + 3H\right) n_{B-L} = \Gamma_{B-L,N} \left(n_N - n_N^{eq}\right) - \Gamma_{B-L,u} \left(u - u^{eq}\right) + \Gamma_{B-L} n_{B-L}. \tag{4.27}$$

At lowest order in relativistic corrections, similarly to (4.7), one gets

$$\Gamma_{B-L,u} = \epsilon \Gamma_0. \tag{4.28}$$

How exactly these corrected rate equations are obtained can be looked up in appendix B.3.

4.3. Radiative corrections

Until now only the decays and inverse decays of heavy neutrinos, so $1 \leftrightarrow 2$ processes have been considered, but naturally there are more processes that affect the neutrino density and therefore the asymmetry n_{B-L} like $2 \leftrightarrow 2$ scattering, $1 \leftrightarrow 3$ decays and virtual corrections to the already treated $1 \leftrightarrow 2$ decays.

Since the density n_{B-L} does not describe actual particles but only the B-L asymmetry relativistic corrections will only affect the neutrino densities or rather the rates associated with these densities. Furthermore it can be shown that the radiative corrections to the number distribution f_N to the change over time, so f_N/dt, for n_N=0 has the following form [16]

$$\left.\frac{\partial f_N}{\partial t}\right|_{f_N=0} = f^{eq}\, \Gamma_0 \frac{M_N}{E_N} \left[a + \frac{p^2}{M_N^2} b + \mathcal{O}\left(\frac{p^4}{M_N^4}\right)\right], \tag{4.29}$$

with a and b the following temperature-dependant coefficients

$$a = 1 - \frac{\lambda T^2}{M_N^2} - |h_t|^2 \left[\frac{21}{2(4\pi)^2} + \frac{7\pi^2}{60}\frac{T^4}{M_N^4}\right] + \left(g_1^2 + 3g_2^2\right) \left[\frac{29}{8\,(4\pi)^4} - \frac{\pi^2}{80}\frac{T^4}{M_N^4}\right] \tag{4.30}$$
$$+ \mathcal{O}\left(g^2\frac{T^6}{M_N^6}, g^3\frac{T^2}{M_N^2}\right),$$
$$b = -\left[|h_t|^2 \frac{7\pi^2}{45} + \left(g_1^2 + 3g_2^2\right)\frac{\pi^2}{60}\right]\frac{T^4}{M_N^4} + \mathcal{O}\left(g^2\frac{T^6}{M_N^6}, g^3\frac{T^2}{M_N^2}\right). \tag{4.31}$$

h_t here denotes the Yukawa coupling of top quarks to the Higgs field, g_1 and g_2 are the U(1) and SU(2) gauge couplings and λ again the Higgs self-coupling.

Plugging equation (4.29) into (4.27) and (4.24) one gets the radiative corrections for Γ_N, Γ_u and Γ_{Nu} by expandig the E_N factor in (4.29) just as done for obtaining the relativistic corrections

and then integrating over the momentum. The results of this procedure that can be looked up in appendix B.4, are at leading order of the respective equation,

$$\Gamma_N = \Gamma_u = a\Gamma_0, \tag{4.32}$$

$$\Gamma_{N,u} = (a - 2b)\Gamma_0. \tag{4.33}$$

One thing interesting to note about the coefficients a and b is the following. The term of lowest order in T in these two coefficients is proportional to $\mathrm{T}^2/\mathrm{M}_N^2$, which corresponds to $\mathcal{O}(p^4)$ because $\mathrm{E}=p^2/M_N \sim \mathrm{T}$ and therefore $\mathrm{p}^2 \sim \mathrm{T}/\mathrm{M}_N$. This would imply that the relativistic corrections should be calculated up to an order of at least p^4, but, as will be obvious later, these corrections of order p^2 are already really small.

5. Numerical results

In order to quantify the results of the previous chapter it is usefull to parameterize the solutions of the rate equations above, especially the solution for the B-L asymmetry described by (4.4) or (4.27) using the so called final efficiency factor κ_f defined via

$$\lim_{z\to\infty} \frac{n_{B-L}}{n_\gamma^{eq}} = \frac{3}{4}\epsilon\kappa_f, \tag{5.1}$$

with $n_\gamma^{eq} = 2\zeta(3)T^3/\pi^2$ the equilibrium density of photons and ϵ the CP-asymmetry parameter. It is now more convenient to rewrite the rate equations in terms of

$$X_i \equiv \frac{n_i}{T^3}, \tag{5.2}$$

with $i = B-L, N$. Using this substitution, one has to consider the transformation [6, Eq. 7.1]

$$\frac{d}{dt}(X_i T^3) + 3Hn_i = \frac{dX_i}{dt}T^3. \tag{5.3}$$

Also, since the limit in (5.1) considers z instead of the time t one has to change the dependence from t to z by using

$$\frac{d}{dt} = \frac{dz}{dt}\frac{d}{z} = \frac{dz}{dT}\frac{dT}{dt}\frac{d}{dz} = -\frac{M_N}{T^2}(-HT)\frac{d}{dz} = zH\frac{d}{dz}. \tag{5.4}$$

Combining all this results in the new, uncorrected rate equations gives

$$zH\frac{dX_N}{dz} = \Gamma_0\left(X_N^{eq} - X_N\right),$$

$$zH\frac{dX_{B-L}}{dz} = \Gamma_0\left[\epsilon\left(X_N - X_N^{eq}\right) + \frac{3}{\pi^2}\left(c_\ell + \frac{c_\phi}{2}\right)z^2K_1(z)X_{B-L}\right],$$

with $N_N^{eq} = 3/8\, z^2K_2(z)$. Now by dividing these rate equations by the factor zH and by using (4.16) one finally arrives at

$$\frac{dX_N}{dz} = zK\left(X_N^{eq} - X_N\right), \tag{5.5}$$

$$\frac{dX_{B-L}}{dz} = zK\left[\epsilon\left(X_N - X_N^{eq}\right) + \frac{3}{\pi^2}\left(c_\ell + \frac{c_\phi}{2}\right)z^2K_1(z)X_{B-L}\right]. \tag{5.6}$$

To be able to relate the result of these rate equations it is useful to express equation (5.6) in terms of

$$N_{B-L} \equiv \frac{n_{B-L}}{n_\gamma^{eq}} = \frac{\pi^2}{2\zeta(3)}X_{B-L}, \tag{5.7}$$

yielding

$$\frac{dN_{B-L}}{dz} = \frac{zK\pi^2}{2\zeta(3)}\epsilon\left(X_N - X_N^{eq}\right) + \frac{3K}{\pi^2}\left(c_\ell + \frac{c_\phi}{2}\right)z^3K_1(z)N_{B-L}. \tag{5.8}$$

Now, in order to finally remove the last unkown parameter in (5.8), namely the CP-asymmetry parameter ϵ one can use the efficiency factor $\kappa(z)$, which is, analogously to (5.1), defined via

$$\frac{n_{B-L}}{n_\gamma^{eq}} = \frac{3}{4}\epsilon\kappa, \tag{5.9}$$

where $\kappa(\infty) = \kappa_f$,to rewrite equation (5.8) resulting in

$$\frac{d\kappa}{dz} = \frac{2\pi^2}{3\zeta(3)} zK\left(X_N - X_N^{eq}\right) + \frac{3}{\pi^2}\left(c_\ell + \frac{c_\phi}{2}\right) z^3 K_1(z) K\kappa. \tag{5.10}$$

The next step will be to introduce the relativistic corrections to these rate equations. For this they have to be normalized in a similar but different way as done in equation (5.2)[6, Eq. (7.9)]:

$$X_u \equiv \frac{M_N^2}{T^5} u = \frac{z^2}{T^3} u, \tag{5.11}$$

with u given in (4.23).

Substituting this for u in the equations (4.22), (4.24) and (4.27) and rewriting the rate equations according to the steps above results in[6, p. 47]

$$\frac{dX_u}{dz} = zK\left(X_u - X_u^{eq}\right), \tag{5.12}$$

$$\frac{dX_N}{dz} = zK\left(X_N^{eq} - X_N\right) + \frac{K}{z}\left(X_u - X_u^{eq}\right), \tag{5.13}$$

$$\frac{d\kappa}{dz} = \frac{2\pi^2}{3\zeta(3)} zK\left[\left(X_N - X_N^{eq}\right) - \frac{K}{z^2}\left(X_u - X_u^{eq}\right)\right] + \frac{3}{\pi^2}\left(c_\ell + \frac{c_\phi}{2}\right) z^3 K_1(z) K\kappa. \tag{5.14}$$

The last thing needed to solve these equations are the two equlibrium distributions X_N^{eq} and X_u^{eq} that are given as

$$X_N^{eq} = \frac{1}{\pi^2} z^2 K_2(z), \tag{5.15}$$

$$X_u^{eq} = \frac{3}{2\pi^2} z^3 K_3(z). \tag{5.16}$$

Their calculation can be looked up in appendix B.5.

Now, after everything needed to solve the rate equation is available, they were solved using a MATLAB code, that can be looked up in appendix B.7. The solution starts at $z = 1$, since there $p \sim M_N$ and therefore the non-relativistic expansion cannot be used for smaller z[5, p. 13]. Also, next to $\kappa(1) = 0$, two sets of initial conditions were used for n_N and u or X_N and X_u respectively, the first one being vanishing X_N and X_u while the second set of initial conditions are thermal ones, thermal meaning that the densities n_N and u start at their corresponding equilibrium values for z=1. Latter is the more physical and realistic scenario because for $K \gtrsim 1$ a reasonable number of right-handed neutrinos will have been produced at z=1[5, p. 13].

Figure 5.1 shows the final efficiency factor plotted against the washout parameter K with and without the relativistic corrections for vanishing und thermal initial conditions, respetively for a temperature ranging from $10^{12} - 10^{13}$GeV. It is easy to see that for small $K \lesssim 4$ the non-relativistic approximation is not viable because for both sets of intial conditions respectively the results of the non-relativistic and the relativistic calculation differ significantly, with the greatest discrepancy appearing for vanishing initial conditions. On the other hand for $K \gtrsim 5$ the differences between initial conditions as well as between non-relativistic and relativistic calculation disappear until the four curves run together for $K \sim 7$. This clearly shows that

for a sufficiently high washout parameter the non-relativistic approximation is a feasible way of describing the evolution of the B-L asymmetry and that higher orders of relativistic corrections are not necessary to be included.

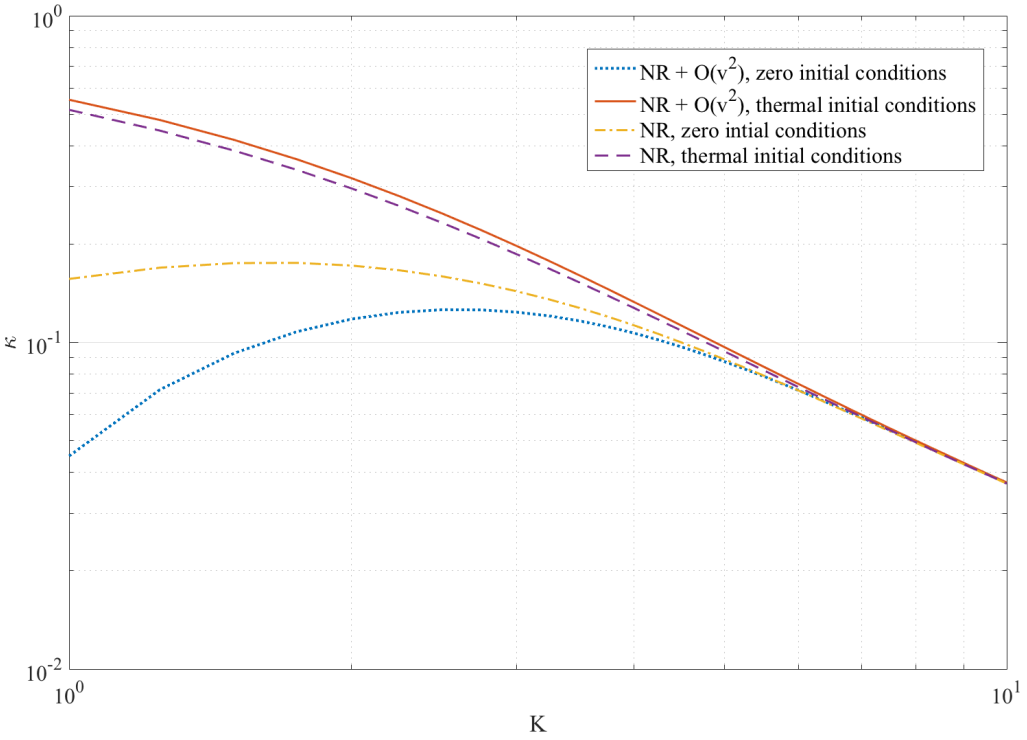

Figure 5.1.: The final efficiency factor depending on the washout strength. The non-relativistic approximation as well as the relativistic corrections are plotted for both zero and thermal initial conditions.The temperature is in a range of $T = 10^8 - 10^{11}$GeV.

The next interesting thing to analyze is how the discrepancies between the non-relativistic approximation and the calculation containing $\mathcal{O}(p^2)$ corrrections evolve with growing K. This is depicted in figure 5.2, where relative difference of these two results is plotted against K for different temperature ranges, while thermal intial conditions were used. For small washout parameters clear differences for the different temperature ranges can be seen, however, even for the highest temperatures of $T > 10^{13}$ GeV this relative difference merely surpasses 10%. This differences then drop rapidly for every temperature until they slowly converge for $K \gtrsim 10$, where the relative error is already well below 1%. For even larger K, namely $K \sim 20$ the relative size of the relativistic corrections is about 0.1% for every shown temperature range. This again, clearly shows, that for a high enough washout parameter K the non-relativistic approach is perfectly viable.

Now figure 5.2 can be used to analyze 5.1 in more detail. As mentioned above the 4 curves in 5.1 run together for $K \sim 7$ and indeed, by looking at the green, dotted curve in 5.2, the relative size of the relativistic corrections is about 1.5% and at the endpoint of 5.1 at K=10 it is 0.7% and therefore the discrepancy is already below 1%.

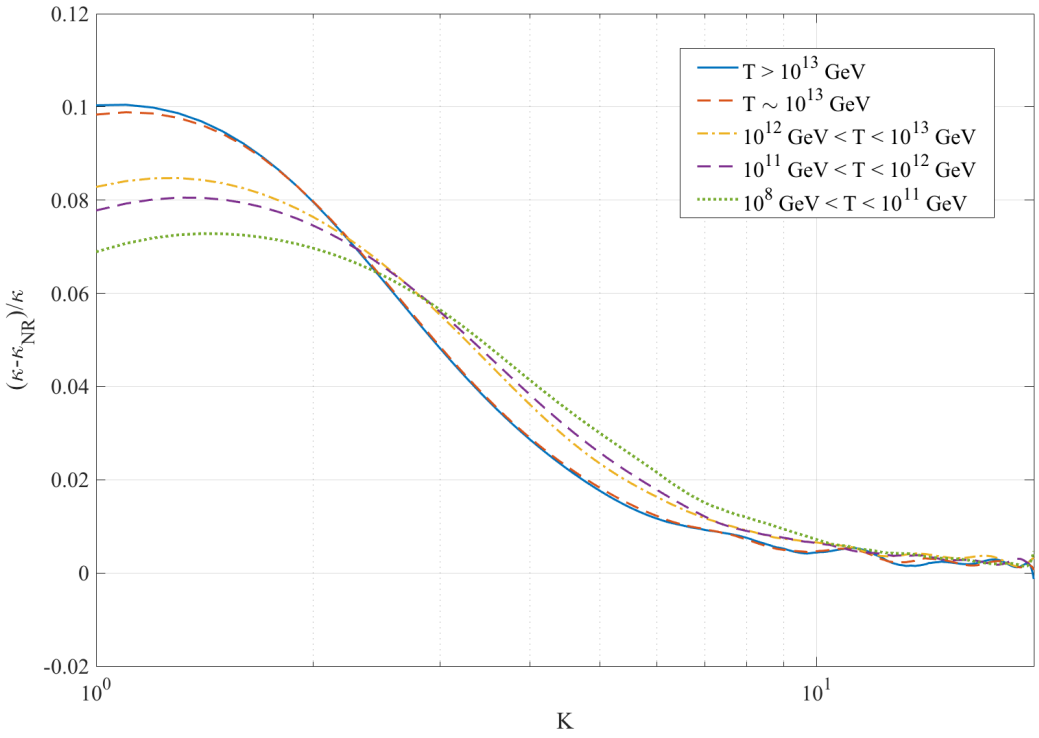

Figure 5.2.: The difference of the non-relativistic approximation and the expansion containing the relativistic corrections normalized to the relativistic solution plotted against the washout parameter for different temperature ranges, corresponding to different values of c_ℓ and c_ϕ. Here thermal initial conditions were used.

Finally the effect of using the correct quantum statistics over classical Boltzmann statistics and vice versa will be studied and examined. During the calculations of the coefficients in the rate equations, more precisely during the calculation of Γ_{B-L} there were two occasions in which the explicit forms of particle distributions had to be used, namely for obtaining the equations (4.12) and (4.13) and even before that for calculating the product $f_\ell f_\phi$.

In the first case quantum statistics were used for leptons and Higgses respectively, yielding the result given in that section. If one uses classical Boltzmann statistics the result changes by a seemingly not that impactful numerical coefficient of $12/\pi^2$, yielding

$$\Gamma_{\text{B-L}} = \frac{1}{4}\left(c_\ell + \frac{c_\phi}{2}\right) z^2 K_1(z) \Gamma_0, \tag{5.17}$$

as given in appendix B.6.

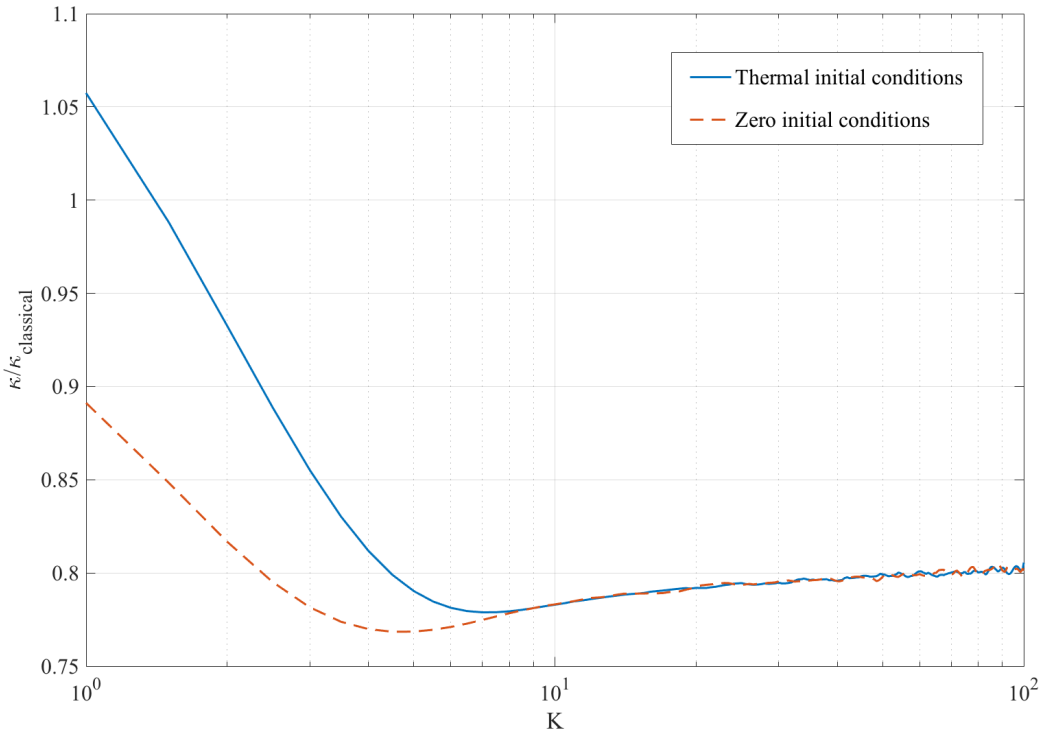

Figure 5.3.: The final efficiency factor determined using the respective quantum stastics to obtain equations for the chemical potentials of leptons and Higgses normalized by the final efficiency factor obtained by using classical Boltzmann statistics for thermal and vanishing initial conditions. $c_l = 1$ and $c_\phi = 0$ were used.

Figure 5.3 however clearly shows that using Boltzmann statistics drastically changes the final efficiency factor. For small K and thermal initial conditions the classical approximation is about 5% smaller than the result obtained using quantum statistics, while for zero initial conditions the classical approximation exeeds the quantum calculation by ∼11%. For growing K the classical approximation grows larger, surpassing the quantum calculation more and more and the deviation peaks at about 24% for K $\simeq$ 5 and zero initial conditions and at about 22% for K $\simeq$ 7 and thermal initial conditions, respectively. For an even larger wash out parameter this deviation slightly lowers until it reaches around 20% for K$\simeq$ 30 for both sets of initial conditions. From this point on $\kappa/\kappa_{classical}$ practically stays constant for growing K. This clearly highlights the importance of using the right statistics, as using classical statistics is a somewhat good approximation only for small wash out parameters, while it completly fails for higher wash out parameters.

On the other hand, because the Higgs particles and leptons are of high energy and the corresponding integrals don't saturate at momenta of order T they can be treated using Maxwell-Boltzmann statistics, in order to calculate the quantity $f_\ell f_\phi - f_{\bar{\ell}} f_{\bar{\phi}}$. Nevertheless it is interesting to see how using the correct quantum statistics and therefore not neglecting their quantum characteristics, affects previous results. As also shown in appendix B.6, this leads the following correction of the coefficient Γ_{B-L}

$$\Gamma_{B-L} = \frac{3}{\pi^2} z^3 \left(\frac{e^{z/2}}{e^{z/2}-1} \frac{c_\phi}{2} + \frac{e^{z/2}}{e^{z/2}-1} c_\ell \right) \int_1^\infty dx \frac{\sqrt{x^2-1}}{e^{zx}-1} \Gamma_0. \tag{5.18}$$

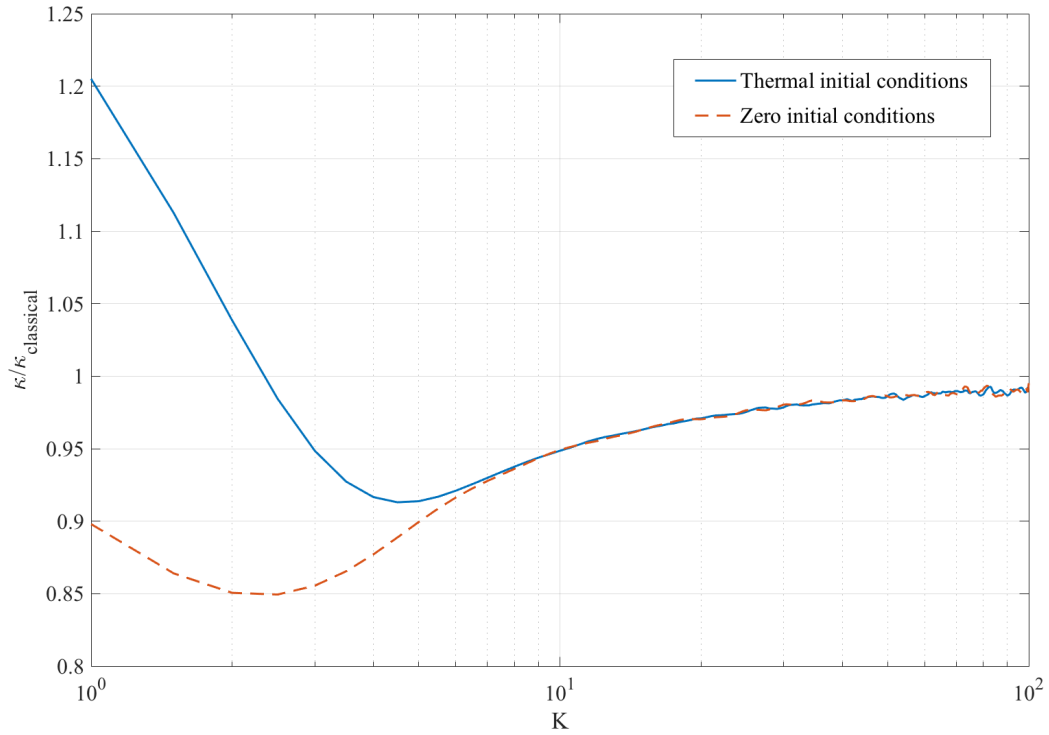

Figure 5.4.: The final efficiency factor determined using only the respective quantum stastics for obtaining $f_\ell f_\phi$ normalized by the final efficiency factor obtained by using classical Boltzmann statistics for thermal and vanishing initial conditions. $c_l = 1$ and $c_\phi = 0$ were used.

Figure 5.4 shows how using (5.18) instead of (4.14) affects the final efficency factor. In the general the course of the graphs is similar to the ones in figure 5.3, however the differences lie in the reached values of the derivation. For K$\sim$1 $\kappa_{classical}$ is about 20% greater than κ for thermal initial conditions and therefore the deviation here is bigger as in 5.3. For zero initial conditions on the other hand the deviation of about 10% is comparable to the one above. Now $\kappa_{classical}$ grows bigger with K and surpasses κ but the drop of $\kappa/\kappa_{classical}$ is not severe as above, as it peaks at around 85% for zero initial conditions and K$\sim$ 2.5, meaning $\kappa_{classical}$ is about 15% bigger than κ. For thermal initial conditions this effect is even smaller with the discrepancy between the to efficiency factor reaching its maximum at around 91% for K$\simeq$ 5. For both sets of initial conditions this effect gets smaller with growing K, so at K=30, the point where a nearly constant difference of about 20% sets in above, the difference is below 2%.

This is a clear sign showing that in the latter of the cases mentioned above using a classical approximation can have a meaningfull impact on the final efficiency for a low wash out parameter, but it slowly gets negligible for higher K in contrast to the first case where the discrepancy between classical and quantum statistics is about 20% even for high K.

Finally, it should be mentioned that the results shown in figure 5.1-5.3 agree with the results depicted in Ref. [5] and [6].

6. Conclusion

In this thesis the basic principles of electroweak baryogenesis and more specifically baryogenesis via leptogenesis were presented. It was shown that for matter antimatter asymmetry creating mechanisms in general the three conditions of baryon number violation, C and CP violation and a departure from the thermal equilibrium, the so called Sakharov conditions, have to be met.

Although the current Standard Model of particle physics could offer everything to meet this conditions in theory, recent experiments have shown that the mass of the Higgs boson is too heavy to induce a electroweak phase transition of sufficiently strong first order or of first order at all. This phase transition of strong first order, however, is needed to ensure that the non-perturbative B violating processes happen outside of thermal equilibrium.

To circumvent this problem the Standard Model is expanded by heavy, right-handed partners of the nowadays observable light neutrinos. By assuming that neutrinos are Majorana particles, so that they are their own antiparticle, these heavy neutrinos could then decay CP violating into leptons and antileptons, respectively, violating lepton number in the process and creating an excess lepton number. For sufficiently high temperatures this lepton number can then be transformed into an excess baryon number by B+L violating processes. This baryon number is then frozen out as soon as the temperature is low enough for the inverse decay to be strongly Boltzmann suppressed. This scenario is known as baryogenesis via leptogenesis.

In addition to this, the rate equations for leptogenesis and the coefficients appearing in the rate equations were obtained in the non-relativistic limit as well as in an expansion including terms of up to first order in relativistic corrections. These equations were then solved in order to compute the B-L asymmetry in the so called strong washout regime, meaning $K > 1$ and the non-relativistic approximation was compared with the relativistic corrections, clearly showing that in the strong washout regime the relative difference between these two is small and that the non-relativistic approximation is a valid one. Also the effect of using different statistics has been computed, showing a far greater influence than the relativistic corrections.

Finally it can be said that a first hint for verifying the model of leptogenesis would be by experimentally proving the Majorana character of neutrinos through processes like the neutrinoless double beta decay. Although no verified event of such a decay has been observed yet, there is still hope that neutrinos are Majorana particles simply because of the tremendous half-life of 10^{24-25} years[17].

Acknowledgements

I want to thank my supervisor Dr. Antonio Vairo for supporting and helping me throughout the whole time I worked on this thesis.

Also thanks to Dr. Mirco Wörmann from the Bielefeld University, whose input cleared up many problems regarding the implementation of the relativistic corrections to the numerical solutions.

A. The Yukawa interaction term

A.1. Feynman rules for the Yukawa interaction

In quantum field theories without Majorana particles the Feynman rules for evaluating Feynman diagrams are acquired from the elements of the so called scattering matrix S, given as [18, Eq. 3.26],

$$\lim_{t_\pm \to \pm\infty} \langle f|U(t_+,t_-)|i\rangle = \langle f|S|i\rangle\,. \tag{A.1}$$

U(t_+,t_-) is an unitary time evolution operator explicitly given by Dyson's formula

$$U(t_+,t_-) = T\exp\left(-i\int_{t_-}^{t_+} dt\; H_{int}(t)\right).$$

In the following $\psi_{x_i} \equiv \psi(x_i)$ will describe an arbitrary fermionic Dirac field, so one can write the time ordering symbol T above in the following way

$$T\psi(x)\psi(y) = \begin{cases} \psi(x)\psi(y) & \text{if } x^0 > y^0 \\ -\psi(y)\psi(x) & \text{if } x^0 < y^0 \end{cases}.$$

Using equation (3.19) for general fields ψ and ϕ, the interaction Hamiltonian can be given as

$$H_{int} = g\int d^3x\overline{\psi}\psi\phi,$$

with g the coupling constant.

Interesting to note is that, given g is small, by expanding the time evolution operator above one can use quantum mechanical pertubation theory up to an arbitrary order.

Now in order to transform the matrix element into a purely algebraic expression, one first has to reorder the fields ψ_1 to ψ_n in a way that the time ordering symbol T is not needed any more. This can be done using the so called Wick's theorem

$$T\left[\psi_1\psi_2\cdots\psi_n\right] =: \psi_1\psi_2\cdots\psi_n + \text{all possible contractions} :\,.$$

The colon notation simply means that the field operators are normally ordered, meaning all creation operators are on the left side of a product, while the annihilation operators are on the right. The exact mathematical expression of the contraction of two field is not of importance here, but can be looked up for example in section 4.2 of [19]. On the other hand the notation and the final result of such a contraction are vital for the following discussion.

$$\text{Contraction of } \psi \text{ and } \overline{\psi} = \overbrace{\psi(x)\overline{\psi}}(y) = \langle 0|T[\psi(x)\overline{\psi}(y)]|0\rangle = iS_F(p).$$

The arrow simply corresponds to the Fourier transformed, since the matrix element above lives in position-space, while it is easier to compute Feynman rules in momentum space. S_F(p) is the fermionic Feynman propagator

$$S_F(p) = \frac{(\not{p}+m)}{p^2+m^2+i\epsilon},$$

where the Feynman slash notation

$$\not{p} = \gamma^\mu p_\mu$$

was used. Now, in order to illustrate what the term 'all possible contractions' in the Wick theorem above means, this theorem will be applied to a time ordered product of two barred and two unbarred fields, which will be given explictily

$$\begin{aligned} T\left[\psi_1\overline{\psi}_2\psi_3\overline{\psi}_4\right] =& :\psi_1\overline{\psi}_2\psi_3\overline{\psi}_4 + \overbracket{\psi_1\overline{\psi}_2}\psi_3\overline{\psi}_4 + \overbracket{\psi_1\overline{\psi}_2\psi_3}\overline{\psi}_4 + \overbracket{\psi_1\overline{\psi}_2\psi_3\overline{\psi}_4} + \psi_1\overbracket{\overline{\psi}_2\psi_3}\overline{\psi}_4 + \\ &+ \psi_1\overbracket{\overline{\psi}_2\psi_3\overline{\psi}_4} + \psi_1\overline{\psi}_2\overbracket{\psi_3\overline{\psi}_4} + \overbracket{\psi_1\overline{\psi}_2}\overbracket{\psi_3\overline{\psi}_4} + \overbracket{\psi_1\overline{\psi}_2\psi_3\overline{\psi}_4} + \overbracket{\psi_1\overline{\psi}_2\psi_3\overline{\psi}_4}: \\ =& :\psi_1\overline{\psi}_2\psi_3\overline{\psi}_4 + \overbracket{\psi_1\overline{\psi}_2}\psi_3\overline{\psi}_4 + \overbracket{\psi_1\overline{\psi}_2\psi_3}\overline{\psi}_4 + \psi_1\overbracket{\overline{\psi}_2\psi_3}\overline{\psi}_4 + \psi_1\overline{\psi}_2\overbracket{\psi_3\overline{\psi}_4} + \\ &+ \overbracket{\psi_1\overline{\psi}_2}\overbracket{\psi_3\overline{\psi}_4} + \overbracket{\psi_1\overline{\psi}_2\psi_3\overline{\psi}_4}: . \end{aligned}$$

In the last step the relations

$$\overbracket{\overline{\psi}(x)\overline{\psi}}(y) = 0, \tag{A.2}$$

$$\overbracket{\psi(x)\psi}(y) = 0, \tag{A.3}$$

were used, having the effect that contracted field are always adjacend to each other in a sense, that to conctraction symbols do not intersect each other. These contractions of just ψ with $\bar{\psi}$ fields can be interpreted as a fermion number flow and therefore the conservation of fermion number. It can be thought of as an incoming particle ψ that becomes an outgoing particle $\bar{\psi}$ after interacting and therefore the fermion number stays the same.

So in order to apply Wicks theorem one has to basically connect two fields pairwise until all possible contractions are performed.

The next important step is to note that only terms with no uncontracted fields contribute to the correlation function above. In the previous example this means that only the last three terms have to be taken into account in order to obtain the corresponding Feynman rules.

Until now only internal contractions, so contractions of two field operators resulting in the internal propagators, where considered. In order to also take the external, so incoming and outgoing, particles into account one has to take a closer look at the initial and final states $|i\rangle$ and $\langle f|$. Because in general these states are not just the vacuum, but (multi-)particle states they must consist of creation and anihilation operators acting on the vacuum state, causing contractions of such operators and the fields to arise. Asuming that the particles are not plane waves but rather localized wave packages one can write the states $|i\rangle$ and $\langle f|$ as[19]

$$\begin{aligned} |i\rangle &= a_1^\dagger a_2^\dagger \cdots b_{n-1}^\dagger b_n^\dagger \left|0\right\rangle, \\ \langle f| &= \langle 0| \, a_1 a_2 \cdots b_{n-1} b_n, \end{aligned}$$

with the annihilation operators a_i, b_i and the creation operators $a_i^\dagger, b_i^\dagger$ for particles and antiparticles, respectively. The subsript i is short for p_i, the particle momentum. In this notations one distinct creation or annihiliation operator can appear twice if two particle with the same momentum are created or destroyed.

Using this and equation (A.1), for a scattering process with a m-particle initial state and a n-particle final state, this results in the following matrix element [20, Eq. 2.2]

$$\left\langle 0 \left| a_1 a_2 \cdots b_{n-1} b_n T\left[(\bar{\psi}\Gamma\psi)\cdots(\bar{\psi}\Gamma\psi)\right] a_{n+1}^\dagger a_{n+2}^\dagger \cdots b_{m-1}^\dagger b_m^\dagger \right| 0 \right\rangle. \tag{A.4}$$

Here the exponential function appearing in the relation above was expanded and only some arbritrary order was chosen, in order to express how the Feynman rules are obtained.

In analogy to the notation in Ref.[20] Γ describes some arbitrary fermionic interaction

$$\bar{\psi}\Gamma\psi = g^i_{abc}\bar{\psi}_a\Gamma_i\psi_b\phi_c,$$

with $\Gamma_i = 1, i\gamma_5, \gamma_\mu\gamma_5, \gamma_\mu, \sigma_{\mu\nu}$, but for the next discussion $\Gamma_i = 1$ will be assumed simply for the sake of clarity.

Applying Wick's Theorem to this new matrix element not only results in the already known propagator terms, but because of the contractions of the fields directly with the creation and annihilation operators one also gets

$$\begin{aligned}
\underbrace{\psi a_i^\dagger} &= \langle 0|\psi(x)a_i^\dagger(p,s)|0\rangle \longrightarrow u(p,s) \text{ incoming particle ,}\\
\underbrace{a_i\bar{\psi}} &= \langle 0|a_i(p,s)\bar{\psi}(x)|0\rangle \longrightarrow \bar{u}(p,s) \text{ outgoing particle ,}\\
\underbrace{\bar{\psi}b_i^\dagger} &= \langle 0|\bar{\psi}(x)b_i^\dagger(p,s)|0\rangle \longrightarrow \bar{v}(p,s) \text{ incoming antiparticle ,}\\
\underbrace{b_i\bar{\psi}} &= \langle 0|b_i(p,s)\psi(x)|0\rangle \longrightarrow v(p,s) \text{ outgoing antiparticle .}
\end{aligned}$$

Here the following expressions for fermion fields

$$\begin{aligned}
\psi &= \sum_{s=\pm 1/2}\int \frac{d^3p}{2(\pi)^3}\,\frac{1}{2E}\left(a(p,s)u(p,s)e^{-ipx} + b^\dagger(p,s)v(p,s)e^{ipx}\right),\\
\bar{\psi} &= \sum_{s=\pm 1/2}\int \frac{d^3p}{2(\pi)^3}\,\frac{1}{2E}\left(a^\dagger(p,s)\bar{u}(p,s)e^{ipx} + b(p,s)\bar{v}(p,s)e^{-ipx}\right),
\end{aligned}$$

and the anti-commutator relations

$$\begin{aligned}
&\{a(p,s), a^\dagger(q,s')\} = \{b(p,s), b^\dagger(q,s')\} = \delta(p-q)\delta_{ss'},\\
&\{a(p,s), a(q,s')\} = \{b(p,s), b(q,s')\} = 0,
\end{aligned}$$

were used to obtain the results above. In this context u, v and their barred versions describe the incoming or outgoing (anti-)particles as seen above, but their exact mathematical expression is of no greater interest here and will therefore not be given.

Shortly summarizing the previous discussion shows that, for Dirac particles, using the matrix element (A.4) one can not only determine the internal propagators needed in most processes but also the spinors of incoming and outgoing particles. So a full set of the needed Feynman rules for Dirac fields was obtained and can directly be used for calculating the scattering matrix elements for various processes.

However, because leptogenesis requires Majorana neutrinos at leas the Feynman rules for exactly this neutrino have to be reiterated. The main difference in obtaining the Feynman rules for Majorana particles in comparison to Dirac particles is that the relations (A.2) and (A.3) do no longer hold and therefore contractions of fields not adjacent to each other are possible. It can be easily seen that the same reasoning of above with incoming and outgoing fermions for Dirac particles can not be applied for Majorana particles because of lepton number non-conserving contractions containing just ψ or $\bar{\psi}$ fields.

This problem can be solved by introducing the charge-conjugated particle

$$\begin{aligned}
\tilde{\psi} &= C\bar{\psi}^T,\\
\bar{\tilde{\psi}} &= -\psi^T C^{-1},
\end{aligned}$$

where C is the charge conjugation operator. The interaction term above then becomes the reversed one

$$\bar{\psi}\Gamma\psi = g^i_{abc}\bar{\psi}_a\Gamma_i\psi_b\phi_c = (-1)g^i_{abc}\psi^T_b\Gamma^T_i\bar{\psi}^T_a\phi_c = g^i_{abc}\bar{\tilde{\psi}}_aC\Gamma^T_iC^{-1}\tilde{\psi}_b\phi_c = g^i_{abc}\bar{\tilde{\psi}}_a\eta_i\Gamma_i\tilde{\psi}_b\phi_c =: \bar{\tilde{\psi}}\Gamma'\tilde{\psi},$$

with the reversed fermion interaction

$$\Gamma' = C\Gamma C^{-1}.$$

In additon the relation

$$C\Gamma_iC^{-1} = \eta_i\Gamma_i,$$

with

$$\eta_i = \begin{cases} +1 & \text{for } 1, i\gamma_5, \gamma_\mu\gamma_5 \\ -1 & \text{for } \gamma_\mu, \sigma_{\mu\nu} \end{cases},$$

was used. Because for Majorana fermions $\tilde{\psi} = \psi$, it is rather easy to notice that the vertex term and the reversed vertex term are the same, $\Gamma' = \Gamma$.

How this untangles intersecting contractions will be shown exemplarily using the following contraction.

$$\bar{\psi}_a\psi_b\,\bar{\psi}_a\psi_b\,\bar{\psi}_a\psi_b.$$

According to the relation above, we now reverse the middle interaction term and therefore get

$$\bar{\psi}_a\psi_b\,\bar{\tilde{\psi}}_b\tilde{\psi}_a\,\bar{\psi}_a\psi_b.$$

Now applying again the contractions, while the same indices as in the original term stay contracted, yields the desired result where all conctracted field are directly next to each other.

$$\bar{\psi}_a\psi_b\,\bar{\tilde{\psi}}_b\tilde{\psi}_a\,\bar{\psi}_a\psi_b. \tag{A.5}$$

This can be applied to an arbitrarlily long string of field operators and therefore any combination of general fermion fields can be transformed in a way that is has the same structure as for Dirac fermions, with the only difference being that some fields may be exchanged with their charge conjugated counterparts. As already mentioned, these kind of interaction terms do not conserve fermion number, however, equation (A.5) having the same structure as for Dirac particles the fermion number flow has to be replaced by something else, namely the so called fermiom flow. This fermion flow plays the role of an orientation of a Feynman diagram. This orientation can be chosen arbitrarily, the resulting matrix element are still the same, regardless of the chosen orientation

The Feynman rules than can be obtained exactly in the same way as for Dirac particles. Using the definition of the charge conjugated fields results in the algebraic expression for the internal propagator given as

$$\langle 0|T[\tilde{\psi}\bar{\tilde{\psi}}]|0\rangle = C\,\langle 0|T[\psi\bar{\psi}]|0\rangle^T\,C^{-1} \longrightarrow CS(p)^TC^{-1} = \frac{(-\not{p} + m)}{p^2 + m^2 + i\epsilon} = S(-p) =: S'(p).$$

Using the explicit expressions for the charge conjugated fields

$$\tilde{\psi} = \sum_{s=\pm 1/2} \int \frac{d^3p}{2(\pi)^3} \frac{1}{2E} \left(a^\dagger(p,s) u(p,s) e^{-ipx} + b(p,s) v(p,s) e^{ipx} \right)$$
$$\bar{\tilde{\psi}} = \sum_{s=\pm 1/2} \int \frac{d^3p}{2(\pi)^3} \frac{1}{2E} \left(a(p,s) \bar{u}(p,s) e^{ipx} + b^\dagger(p,s) \bar{v}(p,s) e^{-ipx} \right)$$

and the exact same anti-commutator relations one gets the analogous results for the external fermion fields;

$$\tilde{\psi} b_i^\dagger = \langle 0 | \tilde{\psi}(x) b_i^\dagger(p,s) | 0 \rangle \longrightarrow u(p,s);$$
$$b_i \bar{\tilde{\psi}} = \langle 0 | b_i(p,s) \bar{\tilde{\psi}}(x) | 0 \rangle \longrightarrow \bar{u}(p,s),$$
$$\bar{\tilde{\psi}} a_i^\dagger = \langle 0 | \bar{\tilde{\psi}}(x) a_i^\dagger(p,s) | 0 \rangle \longrightarrow \bar{v}(p,s),$$
$$a_i \bar{\tilde{\psi}} = \langle 0 | a_i(p,s) \tilde{\psi}(x) | 0 \rangle \longrightarrow v(p,s).$$

Summarizing all these results gives a full set of Feynman rules for Majorana as well as Dirac fermions, as they are given in [20]. For the sake of completeness they will be given here as well. In the following diagramms dotted lines represent a boson field, solid lines without arrows represent Majorana fermions and solid lines with arrows represent Dirac fermions, while the arrow points in the direction of fermion number flow, the thin arrows indicate the fermion flow. The momentum always flows from left to right.

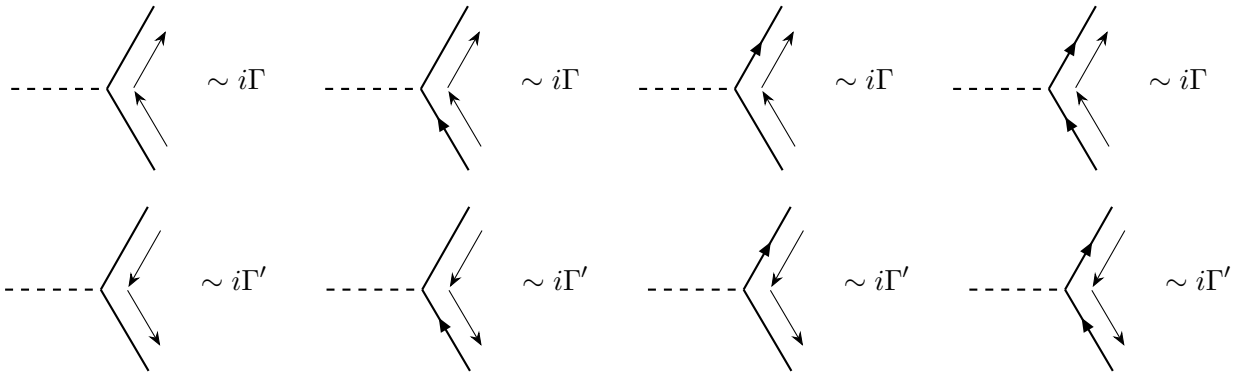

Figure A.1.: Feynman rules for fermionic vertices

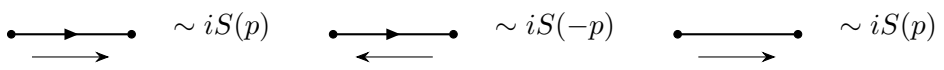

Figure A.2.: Feynman rules for internal fermionic propagators

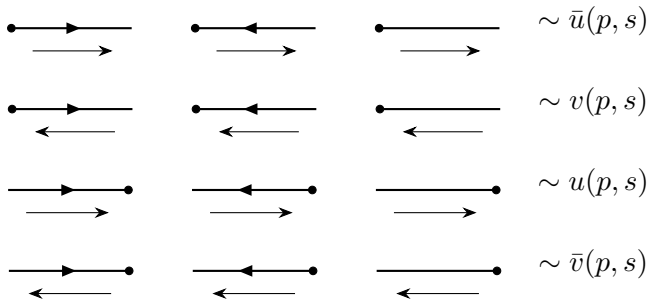

Figure A.3.: Feynman rules for external fermion lines

Now looking at the Lagrangian given in (3.19) one gets the following vertex term for the Feynman diagrams given in figure 3.1:

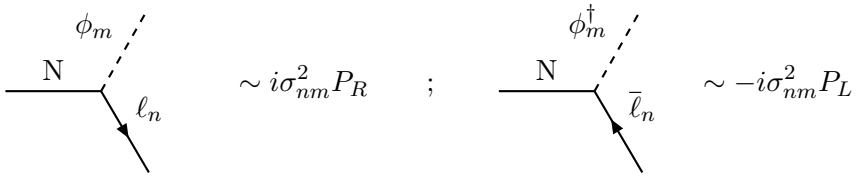

with

$$P_R = \frac{1+\gamma^5}{2}, \qquad P_L = \frac{1-\gamma^5}{2}$$

the chirality operators, with $\gamma^5 = i\gamma^0\gamma^1\gamma^2\gamma^3$, where γ^i denotes the gamma matrices and n, m are isospin indices. This chirality operators here enters the matrix element because the heavy neutrino N, per defnition, has a fixed chirality. The whole matrix element will be given in the following section.

A.2. The tree level decay rate for heavy neutrinos

In this section the heavy neutrion decay rate given in equation (4.6) will be calculated using the tree level diagramms in figure 3.1, which, for the sake of clarity, will be given here once more, but also with arrows showing the arbitrarily chosen orientation

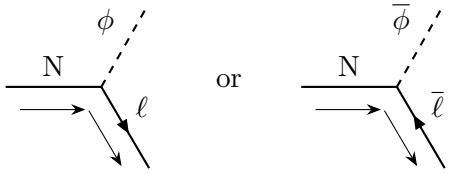

In general the decay rate can be obtained using

$$\Gamma = \int d\Gamma,$$

with the differential decay rate given as

$$d\Gamma = \frac{1}{2M_N} |\mathcal{M}|^2 \frac{d^3p_\ell}{(2\pi)^3 2E_\ell} \frac{d^3p_\phi}{(2\pi)^3 2E_\phi} (2\pi)^4 \delta^4 \left(p_\ell + p_\phi - p_N\right).$$

$|\mathcal{M}|$ denotes the matrix element corresponding to exactly this decay, that can be read off directly from the corresponding Feynman diagram. Now, using the Feynman rules obtained in the previous section one has to first formulate this matrix element in order to be able to evaluate it. Choosing an arbitrary orientation the matrix element for the decay into ϕ and a lepton reads

$$i\mathcal{M} = \bar{u}_{\ell_a}(p_{\ell_a}, s_{\ell_a}) i h_{a1} \sigma^2_{nm} P_R u_N(p_N, s_N),$$

where the subscripts ℓ_a and N describe the lepton of flavor a and heavy neutrino, respectively.

Then the respective absolute square of this matrix element is

$$|\mathcal{M}|^2 = \bar{u}_{\ell_a}(p_{\ell_a}, s_{\ell_a}) h_{a1} P_R u_N(p_N, s_N)\ \bar{u}_N(p_N, s_N) P_L i h^*_{a1} u_{\ell_a}(p_{\ell_a}, s_{\ell_a}),$$

where $\left(\sigma^i\right)^2 = 1$ for $i = 1, 2, 3$ was used.

However, this matrix element only describes the decay of a neutrino with a certain spin into a lepton of another certain spin. In order to generalize this for unknown spins of the lepton as well as of the spin of the heavy neutrino, one has to sum over the final spins of the lepton and average over the initial spin of the neutrino, resulting in

$$|\mathcal{M}|^2 = 2 \cdot \frac{1}{2} \sum_{s_N, s_{\ell_a}} \bar{u}_{\ell_a}(p_{\ell_a}, s_{\ell_a}) h_{a1} P_R u_N(p_N, s_N)\ \bar{u}_N(p_N, s_N) P_L i h^*_{a1} u_{\ell_a}(p_{\ell_a}, s_{\ell_a}).$$

The factor of 2 arises from the fact that general leptons are part of a weak isospin doublet, so there are two possible values for the isospin, or more precise, its third component, namely T_3=-1/2 for the charged leptons e, μ, τ and T_3=1/2 for the corresponding light neutrinos $\nu_{e,\mu,\tau}$. If we just looked at the decay into for example the light neutrinos this factor of 2 has to be omitted since there is only one isospin component T_3 possible. Additionally, the heavy neutrino doesn't contribute to this factor because it is a weak isospin singlet and therefore only T_3=0 is possible.

In the following we only consider the decay into one lepton flavor a=1, taking more flavors into account simply means summing the following result with different coupling constants h_{a1} for each lepton flavor. This results in

$$\begin{aligned}
|\mathcal{M}|^2 &= \sum_{s_N, s_\ell} \bar{u}_\ell(p_\ell, s_\ell) h_{11} P_R u_N(p_N, s_N)\ \bar{u}_N(p_N, s_N) P_L i h^*_{11} u_\ell(p_\ell, s_\ell) = \\
&= |h_{11}|^2 \sum_{s_N, s_\ell} \bar{u}_\ell(p_\ell, s_\ell)_\nu\, P_R^{\nu\mu}\, u_N(p_N, s_N)_\mu\, \bar{u}_N(p_N, s_N)_\alpha\, P_L^{\alpha\beta}\, u_\ell(p_\ell, s_\ell)_\beta = \\
&= |h_{11}|^2 \sum_{s_\ell} \bar{u}_\ell(p_\ell, s_\ell)_\nu\, P_R^{\nu\mu}\, (\not{p}_N + M_N)_{\mu\alpha}\, P_L^{\alpha\beta}\, u_\ell(p_\ell, s_\ell)_\beta = \\
&= |h_{11}|^2 P_R^{\nu\mu}\, (\not{p}_N + M_N)_{\mu\alpha}\, P_L^{\alpha\beta}\, (\not{p}_\ell + M_\ell)_{\beta\nu} = \\
&= |h_{11}|^2 \,\mathrm{Tr}\left[P_R\, (\not{p}_N + M_N)\, P_L\, \not{p}_\ell\right],
\end{aligned}$$

with ν, μ, α, β being spinor indices.

The way this trace was obtained is commonly known as the Casimir trick, which uses the following relation

$$\sum_s u(p, s)\bar{u}(p, s) = \not{p} + m,$$

with m being the mass of the particle.

Because the leptons are relativistic their mass can be neglected, what was done in the last step above.

The trace now simplifies to

$$\begin{aligned}
\mathrm{Tr}\left[P_R\left(\not{p}_N + M_N\right)P_L\not{p}_\ell\right] &= \frac{1}{4}\mathrm{Tr}\left[\left(1+\gamma^5\right)\left(\not{p}_N + M_N\right)\left(1-\gamma^5\right)\not{p}_\ell\right] = \\
&= \frac{1}{4}\left(\mathrm{Tr}\left[\gamma^\mu(p_N)_\mu\gamma^\nu(p_\ell)_\nu\right] + \mathrm{Tr}\left[M\gamma^\mu(p_\ell)_\mu\right] + \right. \\
&+ \mathrm{Tr}\left[\gamma^5\gamma^\mu(p_N)_\mu\gamma^\nu(p_\ell)_\nu\right] + \mathrm{Tr}\left[M\gamma^5\gamma^\mu(p_\ell)_\mu\right] - \\
&- \mathrm{Tr}\left[\gamma^\mu(p_N)_\mu\gamma^5\gamma^\nu(p_\ell)_\nu\right] - \mathrm{Tr}\left[M\gamma^5\gamma^\mu(p_\ell)_\mu\right] - \\
&\left.-\mathrm{Tr}\left[\gamma^5\gamma^\mu(p_N)_\mu\gamma^5\gamma^\nu(p_\ell)_\nu\right] - \mathrm{Tr}\left[M\gamma^5\gamma^5\gamma^\mu(p_\ell)_\mu\right]\right) = \\
&= \frac{1}{4}\mathrm{Tr}\left[\gamma^\mu(p_N)_\mu\gamma^\nu(p_\ell)_\nu\right] - \frac{1}{4}\mathrm{Tr}\left[\gamma^5\gamma^\mu(p_N)_\mu\gamma^5\gamma^\nu(p_\ell)_\nu\right] = \\
&= \frac{1}{2}\mathrm{Tr}\left[\gamma^\mu(p_N)_\mu\gamma^\nu(p_\ell)_\nu\right] = \frac{1}{2}\mathrm{Tr}\left[\not{p}_N\not{p}_\ell\right].
\end{aligned}$$

All of the terms, aside from the first and second to last one, vanished because of the following relations:

$$\mathrm{Tr}\left[\gamma^\mu\right] = 0; \qquad \mathrm{Tr}\left[\gamma^\mu\gamma^\nu\gamma^5\right] = 0; \qquad \mathrm{Tr}\left[\text{odd number of } \gamma\text{'s}\right] = 0$$

The final relation necessary to finally evaluate the trace is

$$\mathrm{Tr}[\gamma^\mu\gamma^\nu] = 4\eta^{\mu\nu},$$

as well as the Minkowski metric $\eta^{\mu\nu}$. Using this one gets the final result for the squared matrix element

$$|\mathcal{M}|^2 = \frac{1}{2}|h_{11}|^2\mathrm{Tr}\left[\not{p}_N\not{p}_\ell\right] = 2|h_{11}|^2(p_N)_\mu(p_\ell)_\nu\eta^{\mu\nu} = 2|h_{11}|^2 p_N p_\ell.$$

In order to rewrite the product of the 4-momentum vectors the decay will be treated in the center of mass system, meaning $p_N = (M_N, \vec{0})$. Additionally, treating the leptons as relativistic particles, so $p_\ell = (|\vec{p}_\ell|, \vec{p}_\ell)$, results in

$$|\mathcal{M}|^2 = 2|h_{11}|^2 p_N p_\ell = 2|h_{11}|^2 M_N|\vec{p}_\ell|.$$

But due to the neutrino not only decaying into leptons but also into anti-leptons this is not the whole contribution to the tree level decay rate. However, looking at figure A.3, the corresponding squared matrix element looks exactly the same and therefore would contribute the same term to the decay rate. This result is not surprising, remembering that CP violation only arises through interference of tree level and one-loop diagrams, thus $\Gamma(N \to \bar{\phi}\ell) = \Gamma(N \to \phi\bar{\ell})$. Plugging both these contribution back into the relation for the total decay rate results in

$$\begin{aligned}
\Gamma &= \frac{1}{2M_N}\int \frac{d^3p_\ell}{(2\pi)^3 2E_\ell}\frac{d^3p_\phi}{(2\pi)^3 2E_\phi}(2\pi)^4 4|h_{11}|^2 M_N|\vec{p}_\ell|\delta^4\left(p_\ell + p_\phi - p_N\right) = \\
&= \frac{1}{8\pi^2}\int \frac{d^3p_\ell}{E_\ell}\frac{d^3p_\phi}{E_\phi}|h_{11}|^2 M_N|\vec{p}_\ell|\delta\left(|\vec{p}_\ell| + |\vec{p}_\phi| - M_N\right)\delta^3\left(\vec{p}_\ell + \vec{p}_\phi\right) = \\
&= \frac{|h_{11}|^2}{8\pi^2}\int \frac{d^3p_\ell}{E_\ell}\frac{1}{E_\phi}|\vec{p}_\ell|\delta\left(2|\vec{p}_\ell| - M_N\right) = \\
&= \frac{|h_{11}|^2}{8\pi^2}\int \frac{d^3p_\ell}{p_\ell}\delta\left(2|\vec{p}_\ell| - M_N\right).
\end{aligned}$$

To get to the third line the 3-momentum delta function was used, resulting in $\vec{p}_N = -\vec{p}_\ell$. Also, since the Higgs particles and leptons are relativistic their energies can be replaced by the absolute value of their momentum. To solve the last remaining integral, one has to use the final delta

function.

$$\begin{aligned}\Gamma &= \frac{|h_{11}|^2}{8\pi^2}\int \frac{d^3p_\ell}{p_\ell}\delta\left(2|\vec{p}_\ell| - M_N\right) = \\ &= \frac{|h_{11}|^2}{2\pi}\int_0^\infty dp_\ell\, p_\ell \delta\left(2|\vec{p}_\ell| - M_N\right) = \\ &= \frac{|h_{11}|^2}{2\pi}\int_0^\infty \frac{dx}{4}\, x\delta\left(x - M_N\right) = \\ &= \frac{|h_{11}|^2}{8\pi}M_N.\end{aligned}$$

B. Detailed calculations

B.1. Integrating the rate equation over phase space

In order to be able to determine Γ_N it is useful to perform the phase space integral over the following equation:

$$\left(\frac{d}{dt}+3H\right)n_N=-\Gamma_N\left(n_N-n_N^{eq}\right).$$

Comparing this to (4.3) one sees that the second term on the right-hand side has already been omitted since it is, as stated above, small enough to be safely neglected.

Now performing the phase space integral results in

$$\begin{aligned}\int\frac{d^3p}{(2\pi)^3}\left(\frac{d}{dt}+3H\right)f_N&=-\int\frac{d^3p}{(2\pi)^3}\,\Gamma_N\left(f_N-f_N^{eq}\right)\\ \Rightarrow\int dp\left(\frac{d}{dt}+3H\right)f_Np^2&=-\int dp\,\Gamma_N\left(f_N-f_N^{eq}\right)p^2.\end{aligned}$$

Using the following partial integration to evaluate the left-hand side

$$\int dp\,p^3\frac{\partial f_N}{\partial p}=\left[p^3f_N\right]_0^\infty-3\int dp\,p^2f_Ndp=-3\int p^2f_N,$$

$$3H\int dp\,f_Np^2=-H\int dp\,p^3\frac{\partial f_N}{\partial p},$$

it follows that

$$\begin{aligned}\int dp\,\left(\partial_t-Hp\partial_p\right)f_Np^2&=-\int dp\,\Gamma_N\left(f_N-f_N^{eq}\right)p^2\\ \Rightarrow\left(\partial_t-Hp\partial_p\right)f_N&=\Gamma_N\left(f_N^{eq}-f_N\right).\end{aligned}$$

B.2. Detailed calculation of Γ_{B-L}

First the rather simple derivation of (4.9) shall be displayed here. For the product of two Boltzman factors one has

$$f_\ell^{eq}f_\phi^{eq}=e^{-\frac{E_\ell-\mu_\ell}{T}}e^{-\frac{E_\phi-\mu_\phi}{T}}=e^{-\frac{E_N-\mu_\ell-\mu_\phi}{T}}=e^{-\frac{E_N}{T}}e^{\frac{\mu_\ell+\mu_\phi}{T}},$$

where the relation $\mathrm{E}_\ell+\mathrm{E}_\phi=\mathrm{E}_\mathrm{N}$ was used.

Expanding this up to first order in the chemical potential results in

$$f_\ell f_\phi\simeq e^{-\frac{E_N}{T}}\left(1+\frac{\mu_\ell+\mu_\phi}{T}\right).$$

Finally putting this togehter for leptons and Higgs particles and using the relation $\mu_X=-\mu_{\bar{X}}$ for the chemical potentials of a particle X and its anti-particle $\bar{X}$ yields the result presented

above,

$$f_l f_\phi - f_{\bar{l}} f_{\bar{\phi}} \simeq e^{-\frac{E_N}{T}} \left(1 + \frac{\mu_l + \mu_\phi}{T} - 1 - \frac{\mu_{\bar{l}} + \mu_{\bar{\phi}}}{T}\right) = 2e^{-\frac{E_N}{T}} \frac{\mu_l + \mu_\phi}{T}.$$

Now, as already explained, in order to relate the chemicial potentials to the density n_{B-L} one has to expand the left-hand side of (4.10) and (4.11) up to first order in the chemical potentials while using Fermi-Dirac and Bose-Einstein distributions instead of Boltzmann statistics, yielding

$$\begin{aligned}
n_\ell - n_{\bar{\ell}} &= g_\ell \int \frac{d^3p}{(2\pi)^3} f_\ell - f_{\bar{\ell}} = \\
&= g_\ell \frac{1}{(2\pi)^3} \int dp\, dcos\theta\, d\phi\, (f_\ell - f_{\bar{\ell}})\, p^2 = \\
&= g_\ell \frac{1}{2\pi^2} \int dp \left(f_\ell\,(\mu_\ell = 0) + \frac{e^{E/T}}{\left(e^{E/T}+1\right)^2 T} \mu_\ell - f_{\bar{\ell}}\,(\mu_{\bar{l}} = 0) - \frac{e^{E/T}}{\left(e^{E/T}+1\right)^2 T} \mu_{\bar{\ell}} \right) p^2 = \\
&= g_\ell \frac{1}{2\pi^2} \int dp\, \frac{2e^{E/T}}{\left(e^{E/T}+1\right)^2 T} \mu_\ell p^2 = \\
&= g_\ell \frac{\mu_\ell}{\pi^2 T} \int_0^\infty dE\, \frac{2e^{E/T}}{\left(e^{E/T}+1\right)^2} E^2 = \\
&= \frac{\mu_\ell T^2}{3}.
\end{aligned}$$

Analogous calculation for the Higgs yields:

$$n_\phi - n_{\bar{\phi}} = \frac{2\mu_\phi T^2}{3}.$$

Here the degrees of freedom $g_\ell = 2 = g_\phi$ were used for leptons as well as for the Higgs.

Solving (4.10) and (4.11) for the chemical potentials results in

$$\begin{aligned}
\mu_\ell &= \frac{3c_\ell}{T^2} n_{B-L}, \\
\mu_\phi &= \frac{3c_\phi}{2T^2} n_{B-L}.
\end{aligned}$$

Plugging all these results into (4.8) one gets the following relation

$$\begin{aligned}
\Gamma_{B-L} &= \frac{3}{8\pi^4} \left(c_\ell + \frac{c_\phi}{2}\right) \frac{M_N}{T^3} \Gamma_0 \int \prod_{a=N,\ell,\phi} \frac{d^3p_a}{E_a} \delta^4\,(p_\ell + p_\phi - p_N)\, e^{-\frac{E_N}{T}} = \\
&= \frac{3}{8\pi^4} \left(c_\ell + \frac{c_\phi}{2}\right) \frac{M_N}{T^3} \Gamma_0 \int \frac{d^3p_N}{E_N} e^{-\frac{E_N}{T}} \left(\int \frac{d^3p_\ell}{E_\ell} \frac{d^3p_\phi}{E_\phi} \delta^4\,(p_\ell + p_\phi - p_N) \right).
\end{aligned}$$

For the sake of minimizing the writing of redundant coefficients we first will evaluate the two body decay phase space in the parentheses above. For simplification the frame of reference used will be the rest frame of the neutrino $\vec{p}_N = 0$.

$$\begin{aligned}
\int \frac{d^3p_\ell}{E_\ell} \frac{d^3p_\phi}{E_\phi} \delta^4\,(p_\ell + p_\phi - p_N) &= \int \frac{d^3p_\ell}{E_\ell} \frac{d^3p_\phi}{E_\phi} \delta\,(E_\ell + E_\phi - M_N)\, \delta^3\,(\vec{p}_\ell + \vec{p}_\phi) = \\
&= \int \frac{d^3p}{E_\ell} \frac{1}{E_\phi} \delta\,(E_\ell + E_\phi - M_N)
\end{aligned}$$

From the first to the second line using the delta distribution for the particle momenta yields $\vec{p} \equiv \vec{p}_\ell = -\vec{p}_\phi$. Also by introducing $\mathrm{E} \equiv E_\ell + E_\phi$ and using spherical coordinates and the following change of integration variables

$$E = E_\ell + E_\phi = \sqrt{M_\ell + p^2} + \sqrt{M_\phi + p^2} \Longrightarrow \frac{dE}{dp} = \frac{p}{E_\ell} + \frac{p}{E_\phi}$$
$$\Longrightarrow dp = \left(\frac{p}{E_l} + \frac{p}{E_\phi}\right)^{-1} dE = \frac{E_\ell E_\phi}{pE_\ell + pE_\phi} dE = \frac{E_\ell E_\phi}{pE} dE,$$

one gets

$$4\pi \int dE\, \frac{p^2}{pE} \delta\left(E - M_N\right) = 4\pi \int dE\, \frac{p}{E} \delta\left(E - M_N\right) = 4\pi \frac{p}{M_N} = 2\pi \frac{M_N}{M_N} = 2\pi$$

In order to evaluate the last integral one has to use the delta distribution, resulting in $\mathrm{E}{=}\mathrm{M_N}$, while the last step uses the fact that leptons and Higgs are relativistic and therefore their energy is $\mathrm{E}_{\ell,\phi} \approx \mathrm{p}$ and in addition that the energy needed for the inverse decay to be possible in the neutrino's rest frame has to be $\mathrm{E}_{\ell,\phi} \approx p = \frac{M_\mathrm{N}}{2}$. Finally plugging this into the original relation for Γ_{B-L} yields

$$\Gamma_{B-L} = \frac{3}{8\pi^4} \left(c_\ell + \frac{c_\phi}{2}\right) \frac{M_N}{T^3} \Gamma_0 \int \frac{d^3 p_N}{E_N} e^{-\frac{E_N}{T}} \cdot 2\pi =$$
$$= \frac{3}{\pi^2} \left(c_\ell + \frac{c_\phi}{2}\right) \frac{M_N}{T^3} \Gamma_0 \int_0^\infty \frac{dp_N}{E_N}\, p_N^2 e^{-\frac{E_N}{T}}.$$

And with the final change of integration variables

$$x = \sqrt{\frac{p_N^2}{M_N^2} + 1} \Longrightarrow p_N = \sqrt{x^2 - 1} M_N \Longrightarrow dp_N = \frac{x}{\sqrt{x^2 - 1}} M_N dx,$$

one gets

$$\Gamma_{B-L} = \frac{3}{\pi^2} \left(c_\ell + \frac{c_\phi}{2}\right) \frac{1}{T^3} \Gamma_0 \int_1^\infty dx\, \frac{\left(x^2 - 1\right) M_N^2}{M_N \cdot x} \cdot \frac{x}{\sqrt{x^2 - 1}} \cdot M_N e^{-zx} =$$
$$= \frac{3}{\pi^2} \left(c_\ell + \frac{c_\phi}{2}\right) z^3 \Gamma_0 \int_1^\infty dx\, \sqrt{x^2 - 1} e^{-zx} =$$
$$= \frac{3}{\pi^2} \left(c_\ell + \frac{c_\phi}{2}\right) z^2 K_1(z) \Gamma_0,$$

where in the last step the definition of the modified Bessel function of the second kind was used:

$$K_n(z) = \frac{\sqrt{\pi}}{\Gamma\left(n + \frac{1}{2}\right)} \left(\frac{1}{2} z\right)^n \int_1^\infty dx\, \left(x^2 - 1\right)^{n - \frac{1}{2}} e^{-zx}.$$

With $\Gamma(n)$ the gamma function.

B.3. Obtaining relativistic corrections to the rate equations

Expanding the factor $1/\mathrm{E}_N$ on the right-hand side of (4.22) by using (4.21) up to order p^2, one gets

$$\left(\frac{\partial}{\partial t} - Hp\frac{\partial}{\partial p}\right) f_N = \Gamma_0 \left(f_N^{eq} - f_N\right) - \frac{\Gamma_0}{2}\left(\frac{p_N}{M_N}\right)^2 \left(f_N^{eq} - f_N\right).$$

Now integrating over p and using the definition of u given in (4.23) the right-hand side simplifies to

$$g_N \int \frac{d^3p}{(2\pi)^3}\left(\Gamma_0 \left(f_N^{eq} - f_N\right) - \frac{\Gamma_0}{2}\left(\frac{p_N}{M_N}\right)^2 \left(f_N^{eq} - f_N\right)\right) = \Gamma_N \left(n_N^{eq} - n_N\right) + \Gamma_{N,u}\left(u - u^{eq}\right)$$

and it can easily be seen that $\Gamma_{N,u} = \Gamma_0$

The left-hand side, however, can be evaluated by performing the steps done in B.1, but in reverse order.

The next thing to do is acquiring the rate equation for u and therefore one has to multiply equation (4.22) with p^2 and integrate over p. At leading order $\left(E_N = M_N\left[1 + \mathcal{O}(p^2)\right]\right)$ in p this yields

$$g_N \int \frac{d^3p}{(2\pi)^3\, M_N}\left(p^2\frac{\partial}{\partial t} - Hp^3\frac{\partial}{\partial p}\right) f_N = \Gamma_0\, g_N \int \frac{d^3p}{M_N}\left(e^{E_N/T} - f_N\right) p^2.$$

Using the following partial integration

$$\begin{aligned} -\int d^3p\, Hp^3 \frac{\partial}{\partial p} f_N &= -4\pi \int dp\, Hp^5 \frac{\partial}{\partial p} f_N = \\ &= -4\pi\left(\left[p^5 f_N\right]_0^\infty - 5\int dp\, p^4 f_N\right) = \\ &= 4\pi \int dp\, 5p^4 f_N = 5\int d^3p\, p^2 f_N \end{aligned}$$

and again the definition of u one easily gets

$$\left(\frac{d}{dt} + 5H\right) u = \Gamma_u \left(u^{eq} - u\right).$$

with $\Gamma_u = \Gamma_0$ at leading order in p.

By performing the same steps as shown in B.1 but applied on equation (4.4) one gets an equation equivalent to (4.5). The last part will be neglected in the following since it doesn't matter considering relativistic corrections.

$$\left(\frac{\partial}{\partial t} - Hp\frac{\partial}{\partial p}\right) f_{B-L} = \frac{M_N \Gamma_{B-L}}{E_N}\left(f_N - e^{-E_N/T}\right)$$

Here the Lorentz invariant phase space was already taken into account.

Analogous to the procedure above one has to only consider the right-hand side of this equation and expanding the factor $1/\mathrm{E}_N$ results in

$$g_N \int \frac{d^3p}{(2\pi)^3}\left(\Gamma_{B-L}\left(f_N - f_N^{eq}\right) - \frac{\Gamma_{B-L}}{2}\left(\frac{p_N}{M_N}\right)^2 \left(f_N - f_N^{eq}\right)\right) = \Gamma_{B-L}\left(n_N - n_N^{eq}\right) - \Gamma_{B-L,u}\left(u - u^{eq}\right).$$

Also easy to see is the following relation:

$$\Gamma_{B-L,u} = \epsilon\Gamma_0$$

B.4. Obtaining radiative corrections to the rate equations

Starting from equation (4.22) one first expresses the number densities through the corresponding distributions and gets

$$\left(\frac{\partial}{\partial t} + 3H\right)\int \frac{d^3p}{(2\pi)^3}\, f_N = \Gamma_N \int \frac{d^3p}{(2\pi)^3}\left(f_N^{eq} - f_N\right) + \frac{\Gamma_{N,u}}{M_N}\int \frac{d^3p}{(2\pi)^3}\frac{p^2}{2M_N}\left(f_N - f_N^{eq}\right).$$

Since the integration variables and range of integration are the same on both sides the integrals and phase space normalization factors can be dropped. Now assuming that these equations hold for $f_N \to 0$ and using (4.29) this simplifies to

$$\begin{aligned} f_N^{eq}\Gamma_0\frac{M_N}{E_N}\left(a + \frac{p^2}{M_N^2}b + \mathcal{O}\left(\frac{p^4}{M_N^4}\right)\right) &= \Gamma_N f_N^{eq} - \Gamma_{N,u}\frac{p^2}{2M_N^2}f_N^{eq} \\ \Rightarrow \Gamma_0\frac{M_N}{E_N}\left(a + \frac{p^2}{2M_N^2}b + \mathcal{O}\left(\frac{p^4}{M_N^4}\right)\right) &= \Gamma_N - \Gamma_{N,u}\frac{p^2}{M_N^2}. \end{aligned}$$

Now again, expanding the $1/E_N$ factor yields

$$\begin{aligned} \Gamma_0\left(1 - \frac{p^2}{M_N^2}\right)\left(a + \frac{p^2}{M_N^2}b + \mathcal{O}\left(\frac{p^4}{M_N^4}\right)\right) &= \Gamma_N - \Gamma_{N,u}\frac{p^2}{2M_N^2} \\ \Rightarrow a\Gamma_0 - (a-2b)\Gamma_0\frac{p^2}{2M_N^2} + \mathcal{O}\left(\frac{p^4}{M_N^4}\right) &= \Gamma_N - \Gamma_{N,u}\frac{p^2}{M_N^2}. \end{aligned}$$

Since equation (4.22) is a relation of order p^2 terms of higher order do not need to be taken into account.

Now simply comparing coefficients of the terms of different order in p yields the already known result

$$\begin{aligned} \Gamma_N =& \Gamma_u = a\Gamma_0, \\ \Gamma_{N,u} =& (a-2b)\Gamma_0. \end{aligned}$$

Using the same procedure on equation (4.24) results in

$$\begin{aligned} &\left(\frac{\partial}{\partial t} + 5H\right)\int \frac{d^3p}{(2\pi)^3}\frac{p^2}{2M_N^2}\, f_N = \frac{\Gamma_u}{M_N}\int \frac{d^3p}{(2\pi)^3}\frac{p^2}{2M_N}\left(f_N - f_N^{eq}\right) \\ &\overset{f_N\to 0}{\Longrightarrow} f_N^{eq}\Gamma_0\frac{M_N}{E_N}\left(a + \mathcal{O}\left(\frac{p^2}{M_N^2}\right)\right) = \Gamma_u\frac{p^2}{M_N^2}f_N^{eq} \\ &\overset{E_N = M_N + \mathcal{O}(p^2)}{\Longrightarrow} \Gamma_u = a\Gamma_0. \end{aligned}$$

Because equation (4.24) is only of order p, one can drop all terms of order p^2 or higher to obtain this result

B.5. Equlibrium densities

In order to be able to solve the rate equations for leptogenesis one has to determine the equlibrium densities X_N^{eq} and X_u^{eq}. Since one consideres $M_N \gg T$, Boltzmann distributions can be used to do so and one gets

$$\begin{aligned}
X_N^{eq} &= \frac{g}{T^3(2\pi)^3}\int d^3p\, e^{-\sqrt{p^2+M_N^2}/T} = \\
&= \frac{1}{\pi^2 T^3}\int_0^\infty dp\, e^{-\sqrt{p^2+M_N^2}/T} p^2 = \\
&= \frac{1}{\pi^2 T^3}\int_{M_N}^\infty dx\, x\sqrt{x^2-M_N^2} e^{-x/T} = \\
&= \frac{1}{\pi^2 T^3}\left(\left[\frac{1}{3}\sqrt{x^2-M_N^2}^3 e^{-x/T}\right]_{M_N}^\infty + \frac{1}{3T}\int_{M_N}^\infty dx\, \sqrt{x^2-M_N^2}^3 e^{-x/T}\right) = \\
&= \frac{M_N^3}{3\pi^2 T^4}\int_{M_N}^\infty dx\, \sqrt{\frac{x^2}{M_N^2}-1}^3\, e^{-x/T} = \\
&= \frac{M_N^4}{3\pi^2 T^4}\int_1^\infty dy\, \sqrt{y^2-1}^3 e^{-zy} = \\
&= \frac{M_N^4}{3\pi^2 T^4}\frac{4}{z^2}\frac{\Gamma(5/2)}{\sqrt{\pi}} K_2(z) = \\
&= \frac{1}{\pi^2} z^2 K_2(z).
\end{aligned}$$

Similarly an expression for X_u^{eq} can be derived:

$$\begin{aligned}
X_u^{eq} &= \frac{g}{T^3(2\pi)^3}\int d^3p\, e^{-\sqrt{p^2+M_N^2}/T} p^3 = \\
&= \frac{1}{\pi^2 T^5}\int_0^\infty dp\, e^{-\sqrt{p^2+M_N^2}/T} p^4 = \\
&= \frac{1}{\pi^2 T^5}\int_{M_N}^\infty dx\, x\sqrt{x^2-M_N^2}^3 e^{-x/T} = \\
&= \frac{1}{\pi^2 T^5}\left(\left[\frac{1}{5}\sqrt{x^2-M_N^2}^5 e^{-x/T}\right]_{M_N}^\infty + \frac{1}{5T}\int_{M_N}^\infty dx\, \sqrt{x^2-M_N^2}^5 e^{-x/T}\right) = \\
&= \frac{M_N^5}{3\pi^2 T^6}\int_{M_N}^\infty dx\, \sqrt{\frac{x^2}{M_N^2}-1}^5\, e^{-x/T} = \\
&= \frac{M_N^6}{3\pi^2 T^6}\int_1^\infty dy\, \sqrt{y^2-1}^5 e^{-zy} = \\
&= \frac{M_N^6}{3\pi^2 T^6}\frac{8}{z^3}\frac{\Gamma(7/2)}{\sqrt{\pi}} K_3(z) = \\
&= \frac{3}{2\pi^2} z^3 K_2(z).
\end{aligned}$$

These two relations can now be used to easily obtain the thermal inital conditions for X_N^{eq} and X_u^{eq}, namely

$$X_N(1) = X_N^{eq}(1) = \frac{1}{\pi^2} K_2(1) \approx 0.165,$$
$$X_u(1) = X_u^{eq}(1) = \frac{3}{2\pi^2} K_3(1) \approx 1.079.$$

At this point it should be mentioned that using these initial is problematic because in order to obtain them Boltzmann statistics, or the assumption of $M_N \gg T$ was used. On the other hand, z=1 implies $M_N = T$, thus classical Boltzmann statistics cannot be used here. We will use these initial conditions nevertheless and treat z=1 as the boundary of the range $M_N \gg T$.

B.6. Differences between quantum and classical statistics

As mentioned in section 5 there are two occurrencens where one can chose classical statistics instead of quantum statistics. The first one covered here will be considering equations (4.12) and (4.13). In section B.2 quantum statistics were used for that particular matter, so here classical statistics will be used. So by expanding up to first order in chemical potentials one gets

$$\begin{aligned}
n_\ell - n_{\bar{\ell}} &= g_\ell \int \frac{d^3p}{(2\pi)^3} \left(f_\ell - f_{\bar{\ell}}\right) = \\
&= g_\ell \frac{1}{(2\pi)^3} \int dp\, dcos\theta\, d\phi \left(f_\ell - f_{\bar{\ell}}\right) p^2 = \\
&= g_\ell \frac{1}{2\pi^2} \int dp \left(f_\ell\left(\mu_\ell = 0\right) + \frac{e^{E/T}}{T}\mu_\ell - f_{\bar{\ell}}\left(\mu_{\bar{l}} = 0\right) - \frac{e^{E/T}}{T}\mu_{\bar{\ell}} \right) p^2 = \\
&= g_\ell \frac{1}{2\pi^2} \int dp\, \frac{2e^{E/T}}{T} p^2 \mu_\ell = \\
&= g_\ell \frac{\mu_\ell}{\pi^2 T} \int_0^\infty dE\, 2e^{E/T}\, E^2 = \\
&= -\frac{4\mu_\ell T^2}{\pi^2},
\end{aligned}$$

where g_ℓ=2 was used. Since Boltzmann statistics do not distinguish between fermions and bosons $n_\ell - n_{\bar{\ell}} = n_\phi - n_{\bar{\phi}}$, yielding

$$\mu_\ell = \frac{\pi^2 c_\ell}{4T^2} n_{B-L},$$
$$\mu_\phi = \frac{\pi^2 c_\phi}{4T^2} n_{B-L}.$$

Plugging this back into (4.8) and following the same calculation as in B.2 then results in

$$\begin{aligned}
\Gamma_{B-L} &= \frac{1}{32\pi^2} \left(c_\ell + \frac{c_\phi}{2}\right) \frac{M_N}{T^3} \Gamma_0 \int \prod_{a=N,\ell,\phi} \frac{d^3p_a}{E_a} \delta^4\left(p_\ell + p_\phi - p_N\right) e^{-\frac{E_N}{T}} = \\
&= \frac{1}{4} \left(c_\ell + \frac{c_\phi}{2}\right) z^2 K_1(z) \Gamma_0.
\end{aligned}$$

On the other hand classical Boltzmann statistics were used to obtain the factor $f_\ell f_\phi - f_{\bar{\ell}} f_{\bar{\phi}}$. How this factor will be corrected using the respective quantum statistics will be shown now.

The product of these two distribution simply yields

$$f_\ell f_\phi = \frac{1}{\left(e^{(E_\ell-\mu_\ell)/T}+1\right)\left(e^{(E_\phi-\mu_\phi)/T}-1\right)}.$$

Now using the following derivatives

$$\frac{\partial}{\partial\mu_\ell} f_\ell f_\phi = \frac{1}{\left(e^{(E_\ell-\mu_\ell)/T}+1\right)^2\left(e^{(E_\phi-\mu_\phi)/T}-1\right)}\,\frac{e^{(E_\ell-\mu_\ell)/T}}{T},$$
$$\frac{\partial}{\partial\mu_\phi} f_\ell f_\phi = \frac{1}{\left(e^{(E_\ell-\mu_\ell)/T}+1\right)\left(e^{(E_\phi-\mu_\phi)/T}-1\right)^2}\,\frac{e^{(E_\phi-\mu_\phi)/T}}{T},$$

this product can be expanded for small chemical potentials up to linear order.

$$f_\ell f_\phi = \frac{1}{\left(e^{E_\ell/T}+1\right)\left(e^{E_\phi/T}-1\right)}\left(1+\frac{e^{E_\phi/T}}{T\left(e^{E_\phi/T}-1\right)}\mu_\phi+\frac{e^{E_\ell/T}}{T\left(e^{E_\ell/T}-1\right)}\mu_\ell\right)+\mathcal{O}(\mu^2)$$

Using this and the relations for the chemical potentials form chapter B.2 one gets

$$f_\ell f_\phi - f_{\bar\ell} f_{\bar\phi} = \frac{6n_{B-L}}{T^3\left(e^{E_\ell/T}+1\right)\left(e^{E_\phi/T}-1\right)}\left(\frac{e^{E_\phi/T}}{e^{E_\phi/T}-1}\,\frac{c_\phi}{2}+\frac{e^{E_\ell/T}}{e^{E_\ell/T}-1}c_\ell\right).$$

where again the relation $\mu_x = \mu_{\bar x}$ was used.

It is also easy to see that by neglecting the ±1 terms in the denominatorsfor high Higgs and lepton energies exactly the result that is obtained by using Maxwell-Boltzmann statistics is reproduced.

Putting this back into (4.8) results in

$$\Gamma_{B-L,q} = \frac{3}{8\pi^4}\,\frac{M_N}{T^3}\Gamma_0\int\frac{d^3p_N}{E_N}\times$$
$$\times\left(\int\frac{d^3p_\ell}{E_\ell}\frac{d^3p_\phi}{E_\phi}\frac{1}{\left(e^{E_\ell/T}+1\right)\left(e^{E_\phi/T}-1\right)}\left(\frac{e^{E_\phi/T}}{e^{E_\phi/T}-1}\,\frac{c_\phi}{2}+\frac{e^{E_\ell/T}}{e^{E_\ell/T}-1}c_\ell\right)\delta^4\left(p_\ell+p_\phi-p_N\right)\right).$$

The addition q to the subscript simply means that this is the quantum corrected rate Γ_{B-L} First the integral in parentheses will be calculated using the 4-momentum delta function.

$$\int\frac{d^3p_\ell}{E_\ell}\frac{d^3p_\phi}{E_\phi}\frac{1}{\left(e^{E_\ell/T}+1\right)\left(e^{E_\phi/T}-1\right)}\left(\frac{e^{E_\phi/T}}{e^{E_\phi/T}-1}\,\frac{c_\phi}{2}+\frac{e^{E_\ell/T}}{e^{E_\ell/T}-1}c_\ell\right)\delta^4\left(p_\ell+p_\phi-p_N\right)=$$
$$=\int\frac{d^3p_\ell}{E_\ell}\frac{1}{E_\phi}\frac{1}{\left(e^{E_\ell/T}+1\right)\left(e^{E_\phi/T}-1\right)}\left(\frac{e^{E_\phi/T}}{e^{E_\phi/T}-1}\,\frac{c_\phi}{2}+\frac{e^{E_\ell/T}}{e^{E_\ell/T}-1}c_\ell\right)\delta\left(E_\ell+E_\phi-M_N\right)=$$
$$=\frac{1}{e^{E_N/T}-1}\int\frac{d^3p_\ell}{p_\ell}\left(\frac{e^{p_\ell/T}}{e^{p_\ell/T}-1}\,\frac{c_\phi}{2}+\frac{e^{p_\ell/T}}{e^{p_\ell/T}-1}c_\ell\right)\delta\left(2p_\ell-M_N\right)$$

The fact that Higgs particles and leptons are relativistic was used and therefore their masses can be neglected. By utilizing the remaining delta function this integral can be calculated as

follows

$$\begin{aligned}
&\frac{1}{e^{E_N/T}-1}\int\frac{d^3p_\ell}{p_\ell}\left(\frac{e^{p_\ell/T}}{e^{p_\ell/T}-1}\,\frac{c_\phi}{2}+\frac{e^{p_\ell/T}}{e^{p_\ell/T}-1}c_\ell\right)\delta\left(2p_\ell-M_N\right)=\\
&=\frac{4\pi}{e^{E_N/T}-1}\int_0^\infty dp\,\left(\frac{e^{p_\ell/T}}{e^{p_\ell/T}-1}\,\frac{c_\phi}{2}+\frac{e^{p_\ell/T}}{e^{p_\ell/T}-1}c_\ell\right)\delta\left(2p_\ell-M_N\right)=\\
&=\frac{2\pi}{e^{E_N/T}-1}\int_0^\infty dx\,\left(\frac{e^{x/2T}}{e^{x/2T}-1}\,\frac{c_\phi}{2}+\frac{e^{x/2T}}{e^{x/2T}-1}c_\ell\right)\delta\left(x-M_N\right)=\\
&=\frac{2\pi}{e^{E_N/T}-1}\left(\frac{e^{M_N/2T}}{e^{M_N/2T}-1}\,\frac{c_\phi}{2}+\frac{e^{M_N/2T}}{e^{M_N/2T}-1}c_\ell\right)=\\
&=\frac{2\pi}{e^{E_N/T}-1}\left(\frac{e^{z/2}}{e^{z/2}-1}\,\frac{c_\phi}{2}+\frac{e^{z/2}}{e^{z/2}-1}c_\ell\right).
\end{aligned}$$

Plugging this back into the original relation for $\Gamma_{B-L,q}$ results in

$$\Gamma_{B-L,q}=\frac{3}{4\pi^3}\,\frac{M_N}{T^3}\left(\frac{e^{z/2}}{e^{z/2}-1}\,\frac{c_\phi}{2}+\frac{e^{z/2}}{e^{z/2}-1}c_\ell\right)\Gamma_0\int\frac{d^3p_N}{E_N}\frac{1}{e^{E_N/T}-1}.$$

This integral cannot be evaluated analytically or even expressed in terms of some known functions as the Bessel function in the case of the uncorrected rate Γ_{B-L}. However, using the same substitution as for calculating Γ_{B-L} we get the final result for the corrections due to the correct quantum statistics

$$\Gamma_{B-L,q}=\frac{3}{\pi^2}\,z^3\left(\frac{e^{z/2}}{e^{z/2}-1}\,\frac{c_\phi}{2}+\frac{e^{z/2}}{e^{z/2}-1}c_\ell\right)I(z)\Gamma_0,$$

with

$$I(z):=\frac{1}{4\pi\,M_N^2}\int\frac{d^3p_N}{E_N}\frac{1}{e^{E_N/T}-1}=\int_1^\infty dx\frac{\sqrt{x^2-1}}{e^{zx}-1}.$$

Using this result one can easily see that for high z of for a high neutrino mass M_N at a fixed temperature and therefore high Higgs and lepton momenta, $\Gamma_{B-L,q}$ changes over to Γ_{B-L}, the result obtained in B.2.

$$\Gamma_{B-L,q}\overset{z\to\infty}{\longrightarrow}\Gamma_{B-L}$$

B.7. MATLAB code

In order to obtain figure 5.1 the following MATLAB code was used:

```
clc


cl = 344/537;
cp = 52/179;

a = 0.1646; %= 1/pi^2*besselk(2,1)
b = 1.0793; %= 3/(2*pi^2)*besselk(3,1);

z = linspace(1,20);      % Range of z over which rate equations are
    solved
y0 = [0 0 0];            % Zero initial conditions for X_(B-L), X_N,
    X_u
y1 = [0 a b];            % Thermal intial conditions for X_(B-L), X_N,
     X_u
x0 = [0 0];              % Zero initial conditions for X_(B-L), X_N
x1 = [0,a];              % Thermal intial conditions for X_(B-L), X_N

 A11=zeros(1,37);        % Matrices of zeroes for later storage of
     data
 A21=zeros(1,37);
 A31=zeros(1,37);
 A41=zeros(1,37);


% The rate equations are solved for each value of K in a range from 1
     to 10
% in steps of 0.25.
% The last calculated data point for each K gets stored in the
    matrices
% defined above

 for K=1:0.25:10

     [z1,N1] = ode15s(@(z,N) density_Rel(z,N,K,cl,cp),z,y0);
     [z2,N2] = ode15s(@(z,N) density_Rel(z,N,K,cl,cp),z,y1);
     A11(1,int16(K*4-3)) = N1(end,1);
     A21(1,int16(K*4-3)) = N2(end,1);
     [z3,N3] = ode15s(@(z,N) density_nonCorr(z,N,K,cl,cp),z,x0);
     [z4,N4] = ode15s(@(z,N) density_nonCorr(z,N,K,cl,cp),z,x1);
     A31(1,int16(K*4-3)) = N3(end,1);
     A41(1,int16(K*4-3)) = N4(end,1);
 end

% Obtained results get smoothed out in order to suppress noise

quinticMA1 = sgolayfilt(A11, 10, 31);
```

```
quinticMA2 = sgolayfilt(A21, 10, 31);
quinticMA3 = sgolayfilt(A31, 10, 31);
quinticMA4 = sgolayfilt(A41, 10, 31);

% Smoothed results are plotted against K

figure(1)
 loglog((1:0.25:10),quinticMA1)
 hold on
 loglog((1:0.25:10),quinticMA2)
 loglog((1:0.25:10),quinticMA3)
 loglog((1:0.25:10),quinticMA4)
 hold off
 xlabel('K')
 ylabel('\kappa')



 % This function defines the rate equation with relativistic
     corrections
 % included

 function ndot = density_Rel(z,N,K,cl,cp)
     nE = 1/pi^2*z^2*besselk(2,z); % X_N in equilibrium
     uE = 3/(2*pi^2)*besselk(3,z)*z^3; % X_u in equilibrium

     ndot=[5.4737*z*K*((N(2)-nE)-1/z^2*(N(3)-uE))-K*z^3*besselk(1,z)
         ...
          *3/pi^2*(cl+cp/2)*N(1);...
          -K*z*(N(2)-nE)+K/z*(N(3)-uE);...
          -K*(N(3)-uE)*z];
 end



% This function defines the rate equation without relativistic
    corrections
% included

function ndot = density_nonCorr(z,N,K,cl,cp)
     nE = 1/pi^2*z^2*besselk(2,z); % X_N in equilibrium

     ndot=[z*5.4737*K*(N(2)-nE)-3/pi^2*(cl + cp/2)*z^3*besselk(1,z)
         *...
          K*N(1);...
           -K*(N(2)-nE)*z];
end
```

Parts of this code which appear analogously in the next codes are not explicitly commented.

Figure 5.2 was created by

```
clc

a = 0.1646; %= 1/pi^2*besselk(2,1)
b = 1.0793; %= 3/(2*pi^2)*besselk(3,1);

z = linspace(1,20);
y1 = [0 a b];
x1 = [0,a];

A13=zeros(1,191);
A23=zeros(1,191);
A33=zeros(1,191);
A43=zeros(1,191);
A53=zeros(1,191);
A63=zeros(1,191);
A73=zeros(1,191);
A83=zeros(1,191);
A93=zeros(1,191);
A103=zeros(1,191);

cl = 1;
cp = 2/3;


for K=1:0.1:20

    [z1,N1] = ode15s(@(z,N) density_Rel(z,N,K,cl,cp),z,y1);
    [z2,N2] = ode15s(@(z,N) density_nonCorr(z,N,K,cl,cp),z,x1);
    A13(1,int16(K*10-9)) = N1(end,1);
    A23(1,int16(K*10-9)) = N2(end,1);
end


cl = 1;
cp = 14/23;


for K=1:0.1:20

    [z1,N1] = ode15s(@(z,N) density_Rel(z,N,K,cl,cp),z,y1);
    [z2,N2] = ode15s(@(z,N) density_nonCorr(z,N,K,cl,cp),z,x1);
    A33(1,int16(K*10-9)) = N1(end,1);
    A43(1,int16(K*10-9)) = N2(end,1);
end


cl = 3/4;
cp = 1/2;

```

```
for K=1:0.1:20

    [z1,N1] = ode15s(@(z,N) density_Rel(z,N,K,cl,cp),z,y1);
    [z2,N2] = ode15s(@(z,N) density_nonCorr(z,N,K,cl,cp),z,x1);
    A53(1,int16(K*10-9)) = N1(end,1);
    A63(1,int16(K*10-9)) = N2(end,1);
end


cl = 78/115;
cp = 56/115;

for K=1:0.1:20

    [z1,N1] = ode15s(@(z,N) density_Rel(z,N,K,cl,cp),z,y1);
    [z2,N2] = ode15s(@(z,N) density_nonCorr(z,N,K,cl,cp),z,x1);
    A73(1,int16(K*10-9)) = N1(end,1);
    A83(1,int16(K*10-9)) = N2(end,1);
end


cl = 344/537;
cp = 52/179;

for K=1:0.1:20

    [z1,N1] = ode15s(@(z,N) density_Rel(z,N,K,cl,cp),z,y1);
    [z2,N2] = ode15s(@(z,N) density_nonCorr(z,N,K,cl,cp),z,x1);
    A93(1,int16(K*10-9)) = N1(end,1);
    A103(1,int16(K*10-9)) = N2(end,1);
end

quinticMA1 = sgolayfilt((A13-A23)./A13, 10, 101);
quinticMA2 = sgolayfilt((A33-A43)./A33, 10, 101);
quinticMA3 = sgolayfilt((A53-A63)./A53, 10, 101);
quinticMA4 = sgolayfilt((A73-A83)./A73, 10, 101);
quinticMA5 = sgolayfilt((A93-A103)./A93, 10, 101);

figure(2)
 semilogx((1:0.1:20),quinticMA1)
 hold on
 semilogx((1:0.1:20),quinticMA2)
 semilogx((1:0.1:20),quinticMA3)
 semilogx((1:0.1:20),quinticMA4)
 semilogx((1:0.1:20),quinticMA5)
 hold off
 xlabel('K')
 ylabel('(\kappa-\kappa_{NR})/\kappa')


```

```
100 function ndot = density_Rel(z,N,K,cl,cp)
101     nE = 1/pi^2*z^2*besselk(2,z);
102     uE = 3/(2*pi^2)*besselk(3,z)*z^3;
103
104     ndot=[5.4737*z*K*((N(2)-nE)-1/z^2*(N(3)-uE))-K*z^3*besselk(1,z)
            *3/pi^2*(cl+cp/2)*N(1);...
105           -K*z*(N(2)-nE)+K/z*(N(3)-uE);...
106           -K*(N(3)-uE)*z];
107 end
108
109 function ndot = density_nonCorr(z,N,K,cl,cp)
110     nE = 1/pi^2*z^2*besselk(2,z);
111
112     ndot=[z*5.4737*K*(N(2)-nE)-3/pi^2*(cl + cp/2)*z^3*besselk(1,z)*K*
            N(1);...
113             -K*(N(2)-nE)*z];
114 end
```

Figure 5.3 was obtained by using

```
clc

cl = 1;
cp = 0;

a = 0.1646; %= 1/pi^2*besselk(2,1)

z = linspace(1,20);
x0 = [0  0];
x1 = [0,a];


A12=zeros(1,199);
A22=zeros(1,199);
A32=zeros(1,199);
A42=zeros(1,199);


for K=1:0.5:100

    [z1,N1] = ode15s(@(z,N) density_nonCorr_classic(z,N,K,cl,cp),z,x0
        );
    [z2,N2] = ode15s(@(z,N) density_nonCorr_classic(z,N,K,cl,cp),z,x1
        );
    A12(1,int16(K*2-1)) = N1(end,1);
    A22(1,int16(K*2-1)) = N2(end,1);
    [z3,N3] = ode15s(@(z,N) density_nonCorr(z,N,K,cl,cp),z,x0);
    [z4,N4] = ode15s(@(z,N) density_nonCorr(z,N,K,cl,cp),z,x1);
    A32(1,int16(K*2-1)) = N3(end,1);
    A42(1,int16(K*2-1)) = N4(end,1);
end

figure(3)
 quinticMA1 = sgolayfilt(A32./A12, 10, 31);
quinticMA2 = sgolayfilt(A42./A22, 10, 31);

 semilogx((1:0.5:100),quinticMA1)
 hold on
 semilogx((1:0.5:100),quinticMA2)
 hold off
 xlabel('K')
 ylabel('\kappa/\kappa_{classical}')

function ndot = density_nonCorr(z,N,K,cl,cp)
    nE = 1/pi^2*z^2*besselk(2,z);

    ndot=[z*5.4737*K*(N(2)-nE)-3/pi^2*(cl + cp/2)*z^3*besselk(1,z)*K*
       N(1);...
          -K*(N(2)-nE)*z];
```

```
47 end
48
49 function ndot = density_nonCorr_classic(z,N,K,cl,cp)
50     nE = 1/pi^2*z^2*besselk(2,z);
51
52     ndot=[z*5.4737*K*(N(2)-nE)-1/4*(cl + cp/2)*z^3*besselk(1,z)*K*N
           (1);...
53           -K*(N(2)-nE)*z];
54 end
```

The following code created 5.4:

```
clc

cl = 1;
cp = 0;

a = 0.1646; %= 1/pi^2*besselk(2,1)

z = linspace(1,20);
x0 = [0  0];
x1 = [0,a];

A12=zeros(1,199);
A22=zeros(1,199);
A32=zeros(1,199);
A42=zeros(1,199);


for K=1:0.5:100

    [z1,N1] = ode15s(@(z,N) density_nonCorr_quantum(z,N,K,cl,cp),z,x0);
    [z2,N2] = ode15s(@(z,N) density_nonCorr_quantum(z,N,K,cl,cp),z,x1);
    A12(1,int16(K*2-1)) = N1(end,1);
    A22(1,int16(K*2-1)) = N2(end,1);
    [z3,N3] = ode15s(@(z,N) density_nonCorr(z,N,K,cl,cp),z,x0);
    [z4,N4] = ode15s(@(z,N) density_nonCorr(z,N,K,cl,cp),z,x1);
    A32(1,int16(K*2-1)) = N3(end,1);
    A42(1,int16(K*2-1)) = N4(end,1);
end

quinticMA1 = sgolayfilt(abs(A12./A32), 10, 31);
quinticMA2 = sgolayfilt(abs(A22./A42), 10, 31);

figure(4)
 semilogx((1:0.5:100),quinticMA1)
 hold on
 semilogx((1:0.5:100),quinticMA2)
 hold off
 xlabel('K')
 ylabel('\kappa/\kappa_{classical}')


function ndot = density_nonCorr(z,N,K,cl,cp)
    nE = 1/pi^2*z^2*besselk(2,z);

    ndot=[z*5.4737*K*(N(2)-nE)-3/pi^2*(cl + cp/2)*z^3*besselk(1,z)*K*N(1);...
          -K*(N(2)-nE)*z];
```

```
47 end
48
49
50 function ndot = density_nonCorr_quantum(z,N,K,cl,cp)
51 nE = 1/pi^2*z^2*besselk(2,z);
52
53 ndot=[z*5.4737*K*(N(2)-nE)-3/pi^2*z^4*exp(z/2)/(exp(z/2)-1)*(cp/2+cl)
       ...
54      *integral(@(x) sqrt(x.^2-1)./(exp(x*z)-1),1,10^1000)*K*N(1);...
55      -K*(N(2)-nE)*z];
56 end
```

Bibliography

[1] S. Sarkar, *Measuring the baryon content of the universe: BBN versus CMB*, astro-ph/0205116.

[2] S. Biondini, *Effective field theories for heavy Majorana neutrinos in a thermal bath*, arXiv:1612.07933 [hep-ph].

[3] J. M. Cline, *Baryogenesis*, [arXiv:hep-ph/0609145v3]

[4] M. Fukugita and T. Yanagida, *Baryogenesis Without Grand Unification*, Phys. Lett. B **174** (1986) 45.

[5] D. Bödeker and M. Wörmann, *Non-relativistic leptogenesis*, JCAP **1402** (2014) 016 [arXiv:1311.2593 [hep-ph]].

[6] M. Wörmann, *Aspects of Nonequilibrium in Leptogenesis* Retrieved 04.07.2017 from http://inspirehep.net/record/1467523/?ln=de

[7] N. Petropoulos, *Baryogenesis at the electroweak phase transition*, [arXiv:hep-ph/0304275]

[8] W. Bernreuther, *CP violation and baryogenesis*, Lect. Notes Phys. **591** (2002) 237 [arXiv:hep-ph/0205279].

[9] Z. Fodor, *Electroweak phase transitions*, Nucl. Phys. Proc. Suppl. **83** (2000) 121 doi:10.1016/S0920-5632(00)91603-7 [arXiv:hep-lat/9909162]

[10] D. Abbaneo *et al.* [ALEPH and DELPHI and L3 and OPAL Collaborations and LEP Electroweak Working Group and SLD Heavy Flavor and Electroweak Groups], *A Combination of preliminary electroweak measurements and constraints on the standard model*, [arXiv:hep-ex/0112021].

[11] M. Drewes, *The Phenomenology of Right Handed Neutrinos*, Int. J. Mod. Phys. E **22** (2013) 1330019 [arXiv:1303.6912 [hep-ph]].

[12] M. Lindner, T. Ohlsson and G. Seidl, *Seesaw mechanisms for Dirac and Majorana neutrino masses*, Phys. Rev. D **65** (2002) 053014 arXiv:hep-ph/0109264v2.

[13] S. Davidson, E. Nardi and Y. Nir, *Leptogenesis*; Phys. Rept. **466** (2008) 105 [arXiv:0802.2962v3 [hep-ph]].

[14] Taanila, O., Helsinki University Department of Physical Sciences. (2008, January). *Neutrinos and thermal leptogenesis*, Retrieved 15.04.2017 from https://helda.helsinki.fi/bitstream/handle/10138/21014/neutrino.pdf;sequence=2

[15] W. Buchmüller, P. Di Bari and M. Plumacher, *Leptogenesis for pedestrians*, Annals Phys. **315** (2005) 305 arXiv:hep-ph/0401240.

[16] M. Laine and Y. Schroder, *Thermal right-handed neutrino production rate in the non-relativistic regime*, JHEP **1202** (2012) 068 [arXiv:1112.1205 [hep-ph]].

[17] R. Arnold *et al.* [NEMO-3 Collaboration], *Measurement of the double-beta decay half-life and search for the neutrinoless double-beta decay of* ^{48}Ca *with the NEMO-3 detector*, Phys. Rev. D **93** (2016) no.11, 112008 [arXiv:1604.01710 [hep-ex]].

[18] Tong, D.,(2016). University of Cambridge Department of Applied Mathematics and Theoretical Physics,*Quantum Field Theory*. Retrieved 18.05.2017 from http://www.damtp.cam.ac.uk/user/tong/qft.html archived at http://www.webcitation.org/6qY4KDfDA

[19] Kopp, J.,(2016, September 16). Johannes Gutenberg Universität Mainz,*Quantum Field Theory - Lecture notes*. Retrieved 15.05.2017 from https://www.staff.uni-mainz.de/jkopp/qft2-2016-material/lecture-notes.pdf archived at http://www.webcitation.org/6qTuXgadV

[20] A. Denner, H. Eck, O. Hahn and J. Kublbeck, *Feynman rules for fermion number violating interactions*, Nucl. Phys. B **387** (1992) 467.

[21] W. Buchmuller, R. D. Peccei and T. Yanagida, *Leptogenesis as the origin of matter*, Ann. Rev. Nucl. Part. Sci. **55** (2005) 311 [hep-ph/0502169].

[22] Perepelitsa, D. V., Columbia University Department of Physics. (2008, November 25). *Sakharov Conditions for Baryogenesis*. Retrieved 10.02.2017 from http://phys.columbia.edu/ dvp/dvp-sakharov.pdf archived at http://www.webcitation.org/6oB6H9FQv

[23] P. Di Bari, *Beyond the Standard Model with leptogenesis and neutrino data*, arXiv:1612.07794 [hep-ph].

[24] J. Ellis, *TikZ-Feynman: Feynman diagrams with TikZ*, Comput. Phys. Commun. **210** (2017) 103 arXiv:1601.05437 [hep-ph].

[25] R. Kleiss, I. Malamos and G. van den Oord, *Majoranized Feynman rules*, Eur. Phys. J. C **64** (2009) 387 [arXiv:0906.3388 [hep-ph]].